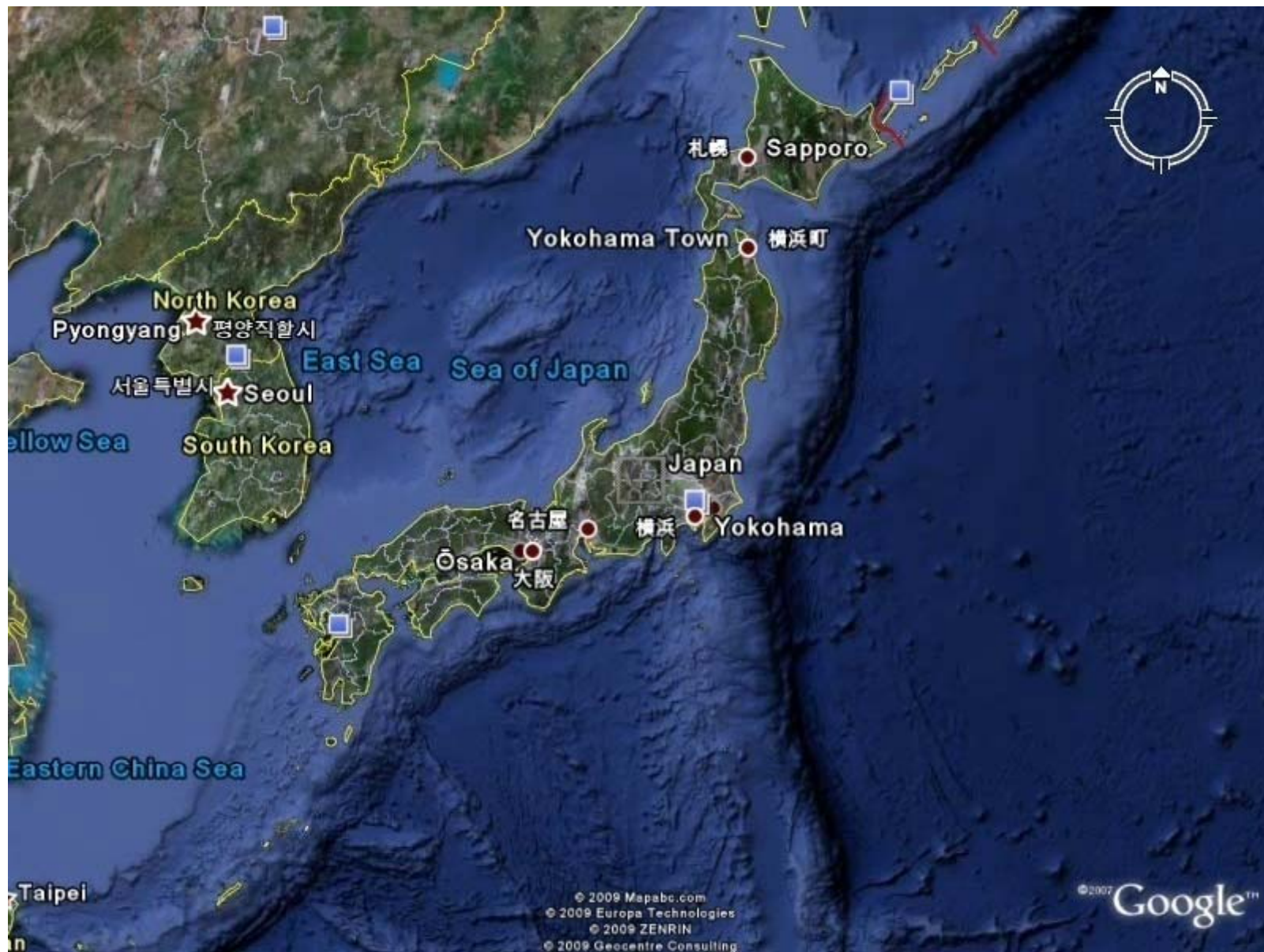


CHARGE DENSITY STUDY

how & why

Finn Krebs Larsen
Aarhus University,
Denmark



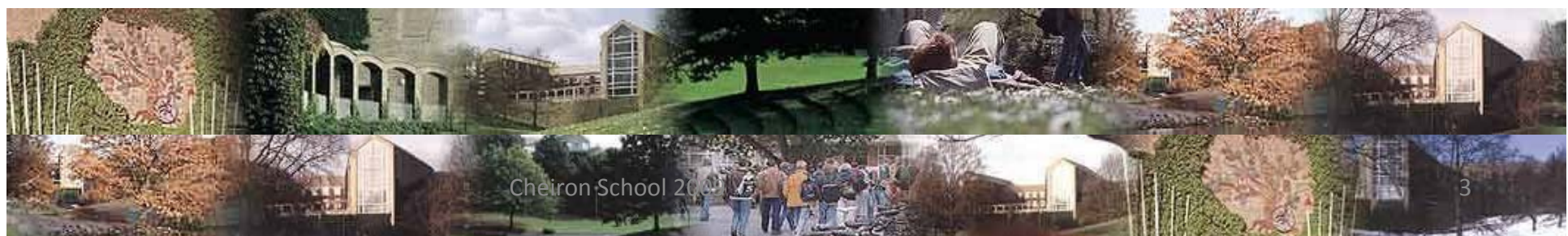
Aarhus University,



Denmark

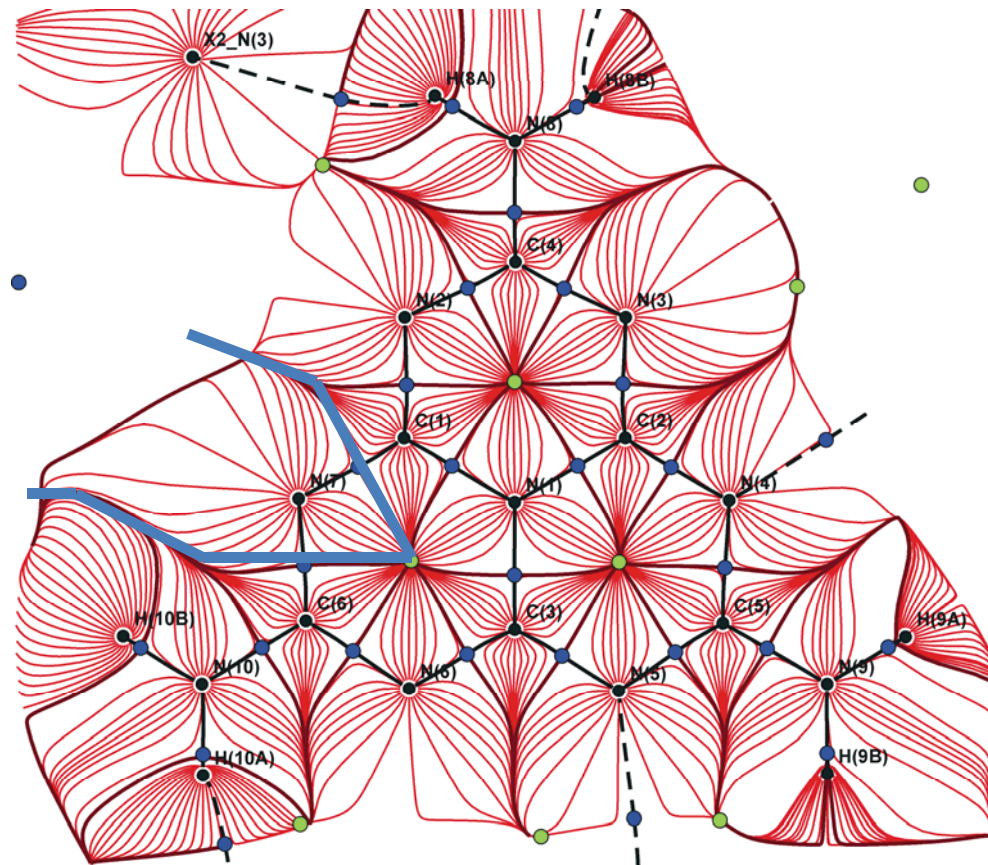
Department of Chemistry

9 Profs.
22 Associate Profs.
4 Assistant Profs.
38 techs/Adm
60 Post docs
~100 Phd Students
~80 Masters students
>200 undergrad. majors



More than just pretty pictures

In 2D



Outline

Part 1

- **Modelling in crystallography**
 - a) Atomic Thermal Motion
 - b) Electron Density Distribution
- **Experimental requirements & challenges**

Part 2

- **Selected examples from our library of structures**
 - 1) Transition metal complex. Jahn-Teller effect.
 - Comparison with theory. Topological analysis
 - 2) Thermoelectric materials. CoSb₃
 - 3) Hydrogen bonding
 - 4) Coordination polymers
 - 5) Chrome wheel complexes
- **Conclusions**

$$F(\mathbf{H}) = \int \rho(\mathbf{r}) \exp(2\pi i \mathbf{H} \cdot \mathbf{r}) d\mathbf{r}$$

- The **structure factor** is the Fourier transform of the periodic electron density.
- Discrete values for $\mathbf{H} = h \cdot \mathbf{a}^* + k \cdot \mathbf{b}^* + l \cdot \mathbf{c}^*$ for integer values of h , k , and l in reciprocal space

Experimental Structure Factor

$|F_{\text{obs}}|$ can be deduced by applying corrections to the **integrated reflectivity, $R(\mathbf{H})$** , which can be measured in a diffraction experiment.

$$R(\mathbf{H}) = k \cdot L \cdot P \cdot T_{\text{absorb}} \cdot E_{\text{extinc}} \cdot |F_{\text{obs}}|^2$$

K : scale factor

L·P : Lorentz-Polarization correction

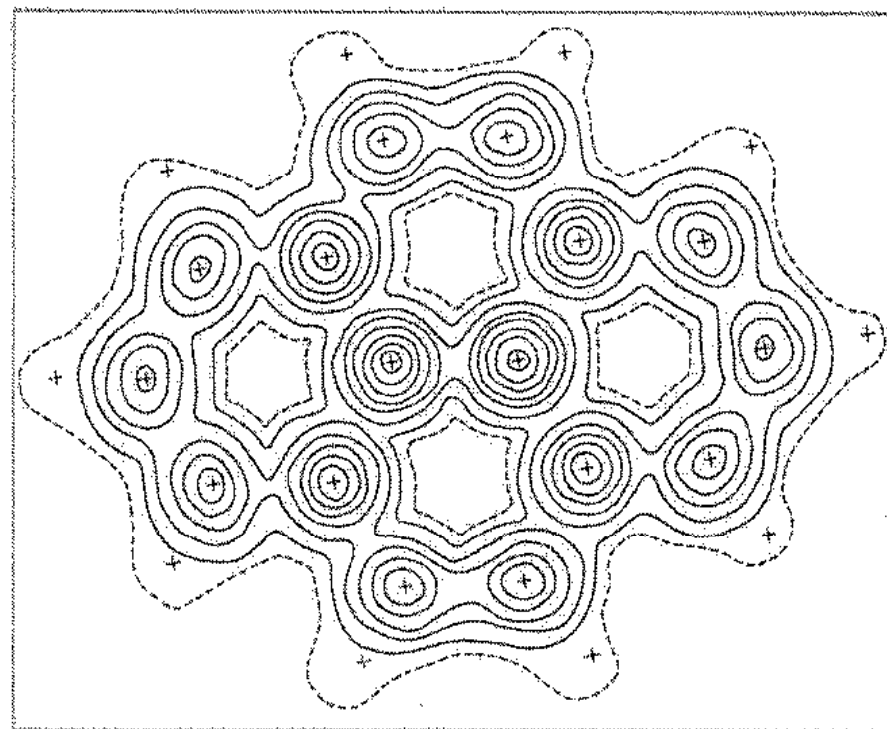
T_{absorb} : absorption correction

E_{extinc} : extinction correction

CRYSTALLOGRAPHY

Solve the structure and find the phase → F_{obs}

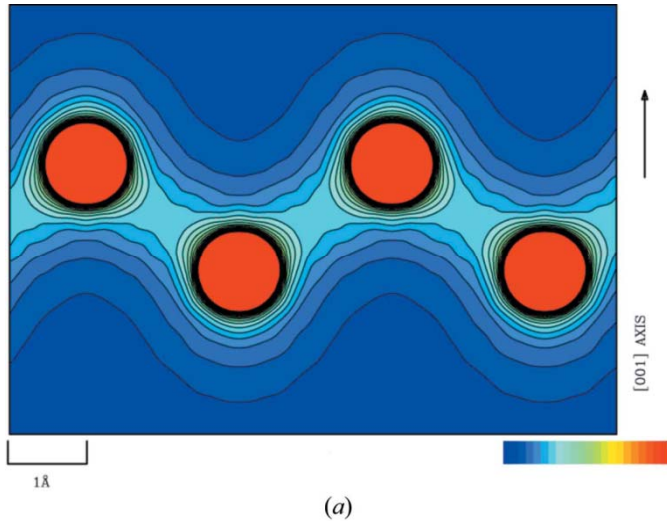
Total density : $\rho(\mathbf{r}) = \frac{1}{V_{uc}} \sum_{\mathbf{H}} \left(\frac{\mathbf{F}_{obs}(\mathbf{H})}{k} \right) \exp(-2\pi i \mathbf{H} \cdot \mathbf{r})$



Pyrene, C₁₆H₁₀

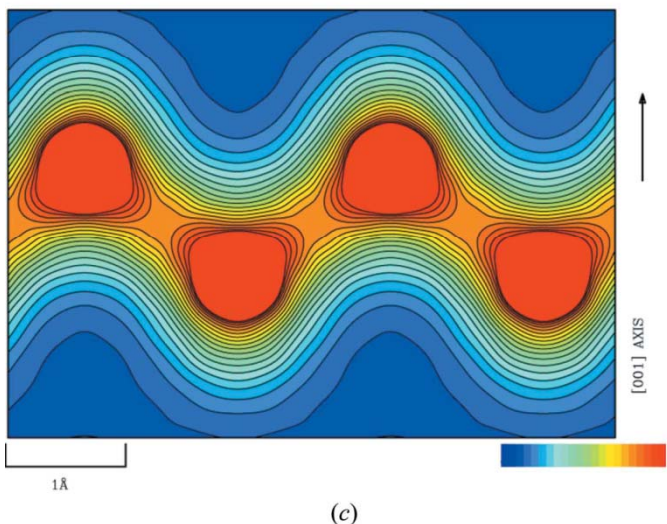
Hazell, Larsen and Lehmann
Acta Cryst. (1972). B28, 2977-2984

MEM charge density



Nishibori, Sunaoshi, Yoshida, Aoyagi, Kato,
Takata and Sakata
Acta Cryst. (2007). **A63**, 43-52

Si at 100 K
measured at beamline BL02B2 at Spring-8



Diamond at 100 K
measured at beamline BL02B2 at Spring-8

Modelling

IAM (independent atom model)

$$F(\mathbf{H}) = \sum_{i=1}^{nat} f_i(\mathbf{H}) \exp(2\pi i \mathbf{H} \cdot \mathbf{r}_i) T_i$$

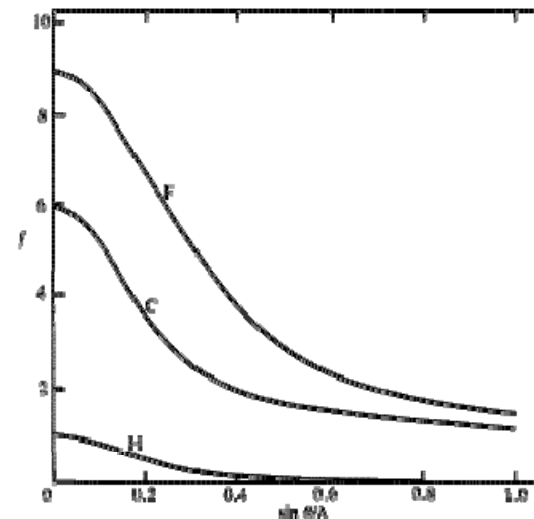
$$f(\mathbf{S}) = \int \rho_{at}(\mathbf{r}) \exp(2\pi i \mathbf{S} \cdot \mathbf{r}) d\mathbf{r}$$

Atomic

Scattering factor : f_i

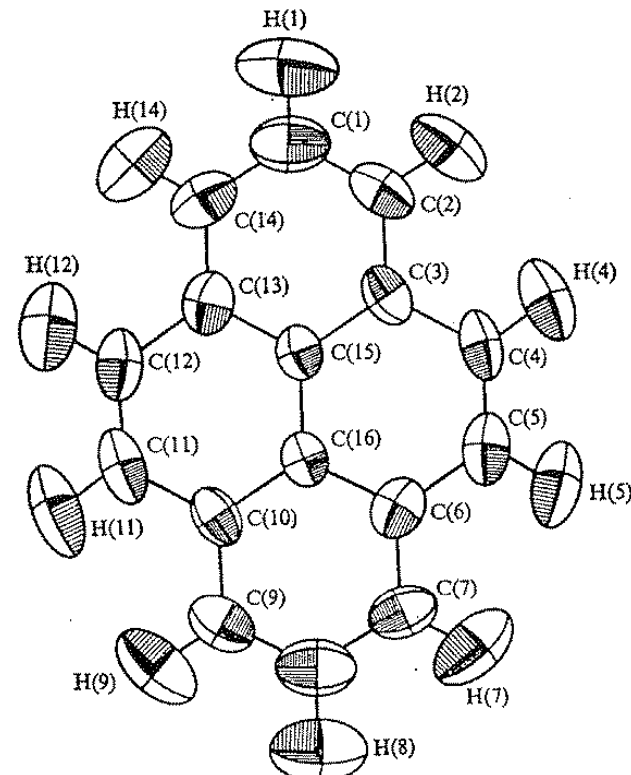
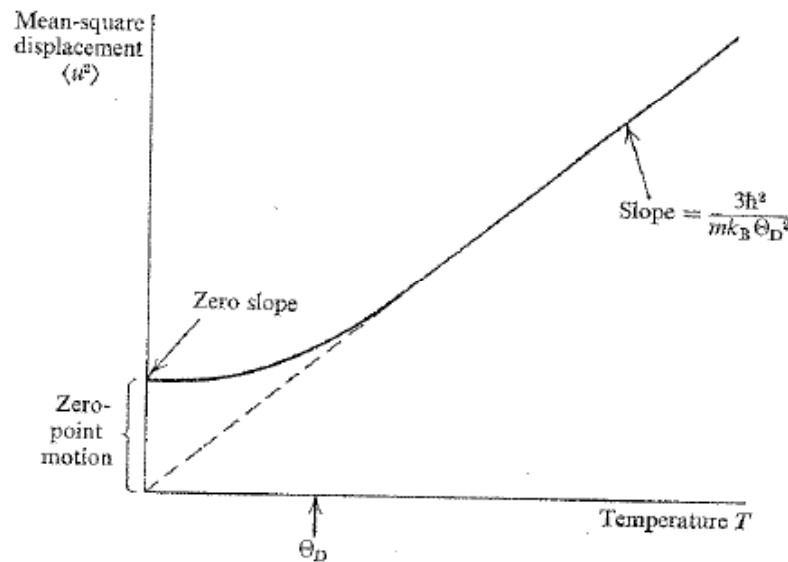
Coordinates : $\mathbf{r}_i = x_i, y_i, z_i$

Temperature factor : T_i



Atomic Thermal Motion

- Harmonic , isotropic Harmonic, anisotropic
 - Debye approximation



- $T_{harm,iso} = \exp(-8\pi^2 \langle u_j^2 \rangle) (\sin\theta/\lambda)^2$

Atomic Temperature factor

$$T_j(H) = T_{j,\text{harmonic}}(H) \cdot T_{j,\text{anharmonic}}(H)$$

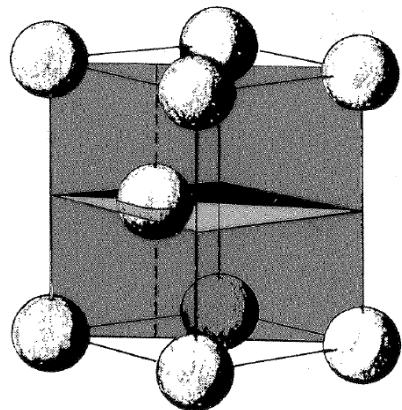
$$\begin{aligned} T_{j,\text{harmonic}} = T_{j,\text{aniso}} &= \exp(-2\pi^2(U_{11}h^2a^{*2} + U_{22}k^2b^{*2} + U_{33}l^2c^{*2} \\ &\quad + 2U_{23}klb^*c^* + 2U_{13}hla^*c^* + 2U_{12}hka^*b^*)) \end{aligned}$$

$$\begin{aligned} T_{j,\text{anharmonic}} &= \exp(-2\pi^2 (1 - i4/3\pi^3 C^{jkl} h_j h_k h_l + \\ &\quad 2/3\pi^4 D^{jklm} h_j h_k h_l h_m)) \end{aligned}$$

cubic and quartic Gram-Charlier expansion

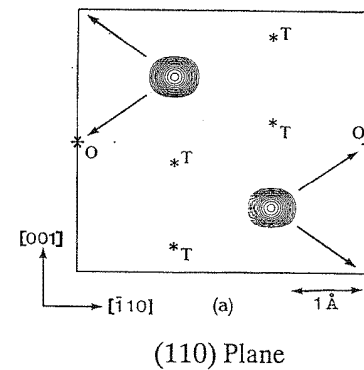
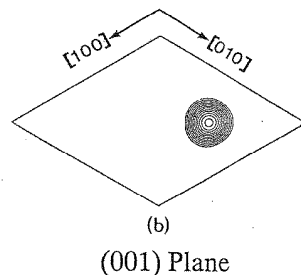
Thermal parameters

Beryllium hcp structure



Nuclear density distribution

Anharmonic motion



- Atomic Temperature factor $T(H)$
- harmonic, isotropic :
- harmonic, anisotropic :
- Anharmonic, cubic
- Anharmonic, quartic

Number of thermal parameters

1

6

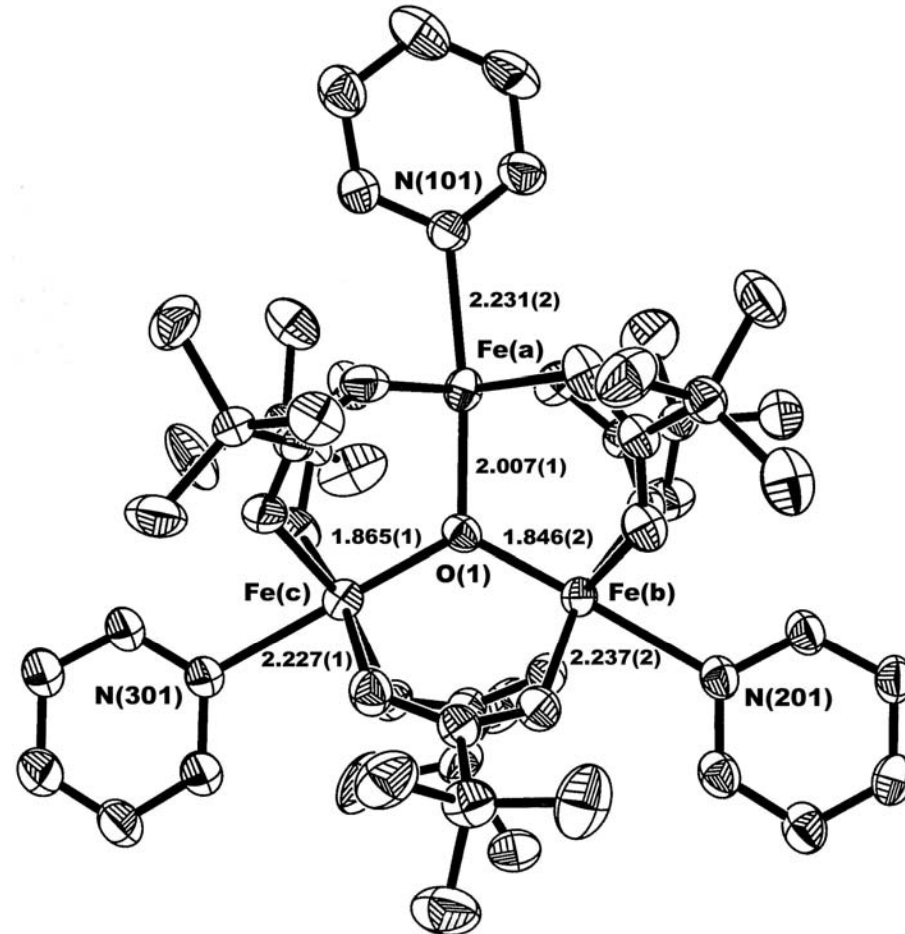
6 + 10

6 + 10 + 15

Normal structure determination (IAM)

"Result" of a crystallographic structure determination is the usual ORTEP-drawing which shows the **NUCLEAR PROBABILITY DENSITY FUNCTION**

The IAM model is only concerned with the core electrons/nuclear density. It works surprisingly well!

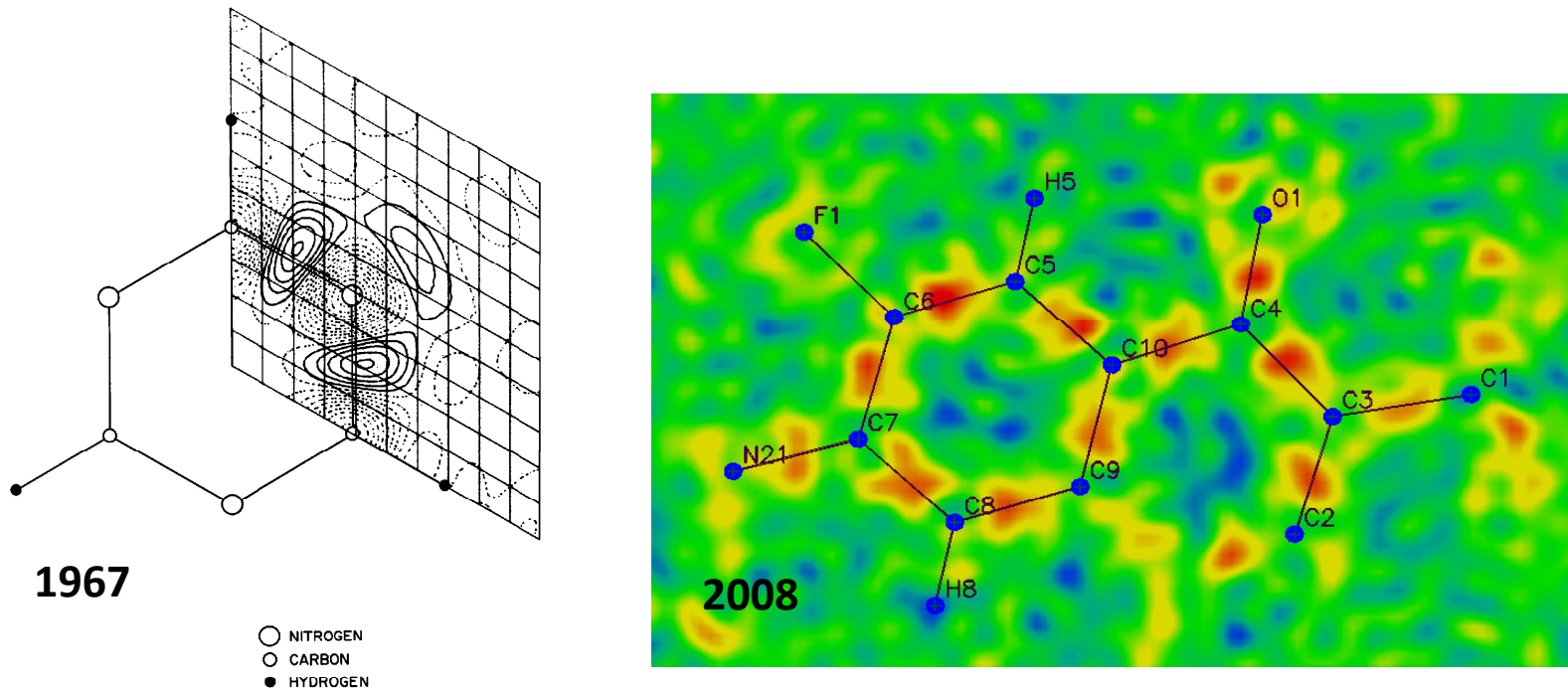


Structure Refinement

- Least-squares minimisation of
- $\sum w(F_{\text{obs}}^2 - F_{\text{calc}}^2)^2 = \text{minimum}$
- Refine scale factor, positional, and thermal atomic parameters.
- Then check the difference Fourier !

The IAM model

Difference Fourier maps: $\Delta\rho(\mathbf{r}) = \frac{1}{V_{uc}} \sum_{\mathbf{H}} \left(\frac{\mathbf{F}_{obs}(\mathbf{H})}{k} - \mathbf{F}_{calc}(\mathbf{H}) \right) \exp(-2\pi i \mathbf{H} \cdot \mathbf{r})$



Expanding the atomic model

Stewart (1969): Develops generalized scattering factors from orbital products and envisions their use in modeling of experimentally measured X-ray structure factors as electron density studies. Suggests that the effects are significant enough to be measured.

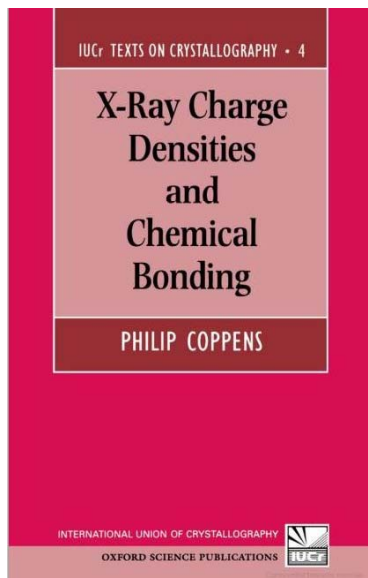
Hansen-Coppens (1978): Builds on the work by Stewart, but uses a modified version where the angular part of the density functions are based on spherical harmonic functions :

$$\rho = \text{core} + \text{valence} + \text{deformation (bonding, lone pair etc)}$$

$$\rho(\mathbf{r}) = P_c \rho_c + P_v \rho_v(kr) k^3 + \sum_{l=0}^{l_{\max}} R_l(k'r) k'^3 \sum_{m=0}^l P_{lm\pm} d_{lm\pm}(\theta, \phi)$$

Sources

Part 1

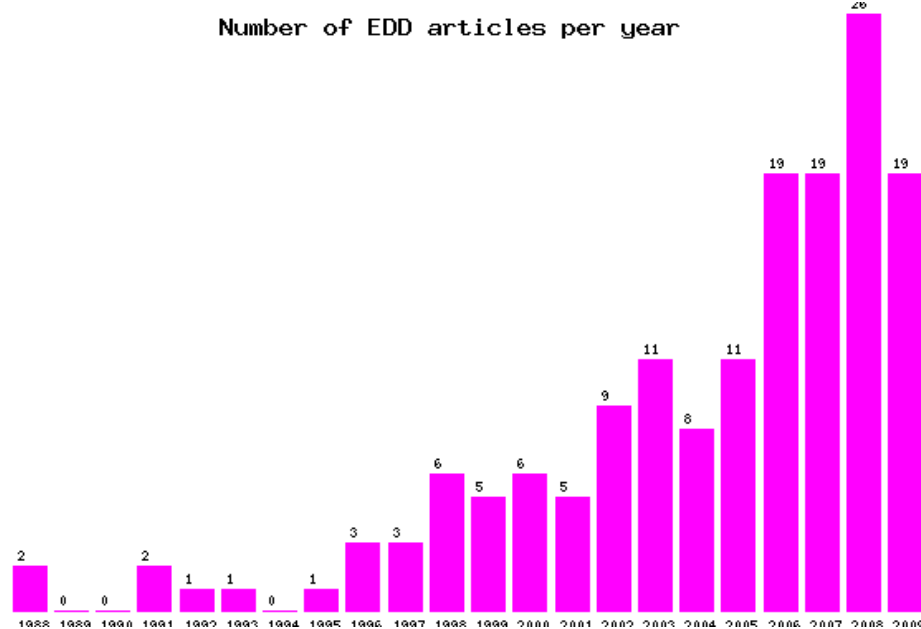


Philip Coppens:
"X-ray charge densities
and Chemical Bonding"



<http://xd.chem.buffalo.edu/>

Part 2



<http://www.chem.au.dk/~uorg/cddb>

Characteristics of spherical harmonics

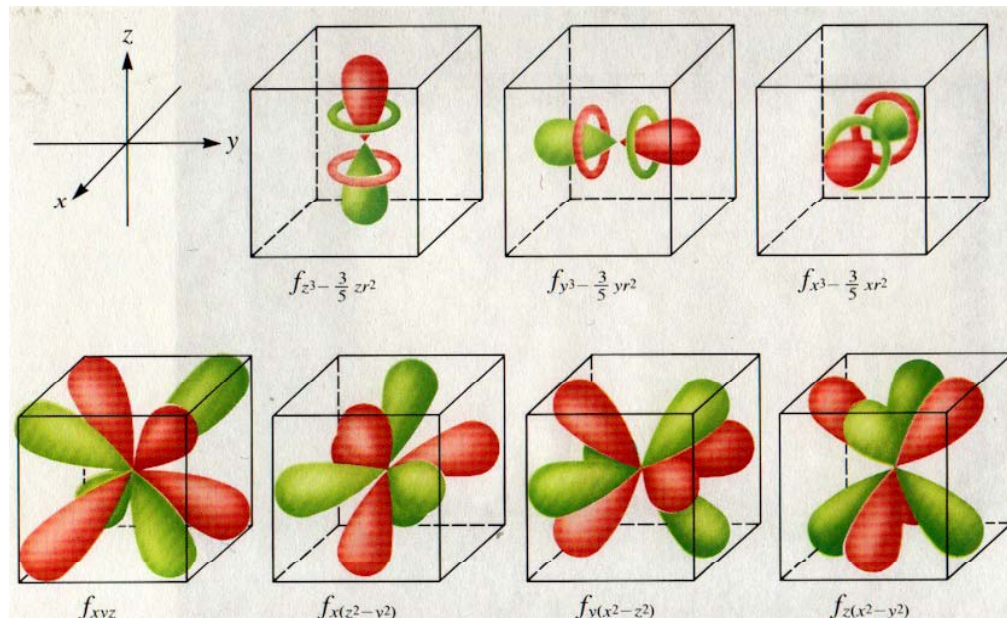
Hansen-Coppens structure factor:

$$F(\mathbf{H}) = \sum_{i=1}^{nat} f_i(\mathbf{H}) \exp(2\pi i \mathbf{H} \cdot \mathbf{r}_i) T_i \rightarrow$$

$$F(\mathbf{H}) = \sum_i \left(P_c f_{c,i} + P_v f_{v,i} (\mathbf{H}/\kappa) \kappa^3 + 4\pi \sum_{l=0}^{l_{\max}} \sum_{m=0,l} P_{lm\pm} i^l \langle j_l(H/\kappa') \rangle d_{lm\pm}(\beta, \gamma) \right) \exp(2\pi i \mathbf{H} \cdot \mathbf{r}_i) T_i$$

Ex. f-orbitalic functions
(octopoles):

Charge is moved from red
to green if the multipole is
populated



Density Parameters for s, p, d, and f-orbital functions

Number of charge density parameters in multipole model

Monopole : 1

Dipoles : 3

Quadrupoles : 5

Octopoles : 7

Hexadecapoles : 9

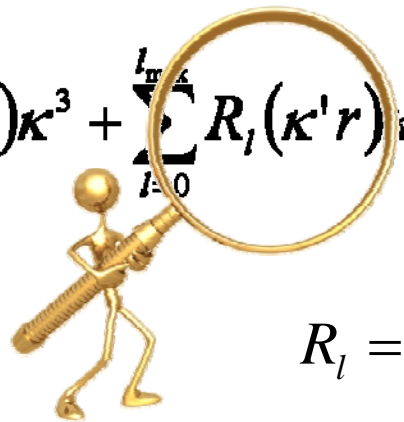
In total pr atom : 9 - 25

Expansion or contraction of the atomic electron density are described with Kappa parameters via the radial function

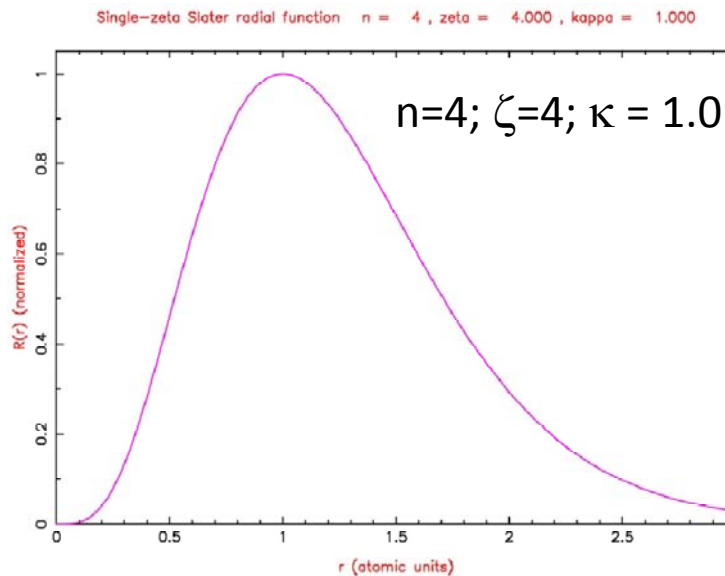
The radial function

$$\rho(\mathbf{r}) = P_c \rho_c + P_v \rho_v(\kappa r) \kappa^3 + \sum_{l=0}^{l_{\max}} R_l(\kappa' r) \kappa'^3 \sum_{m=0}^l P_{lm\pm} d_{lm\pm}(\theta, \phi)$$

Nodeless, normalized, density functions:



$$R_l = \kappa'^3 \frac{\zeta^{n_l+3}}{(n_l + 2)!} (\kappa' r)^{n_l} \exp(-\kappa' \zeta_l r)$$



Experimental implications

Besides a scale factor electron density modelling requires refinement of many parameters per atom

Positional parameters	3
Thermal parameters	6 → 31
Charge density parameters	9 → 25

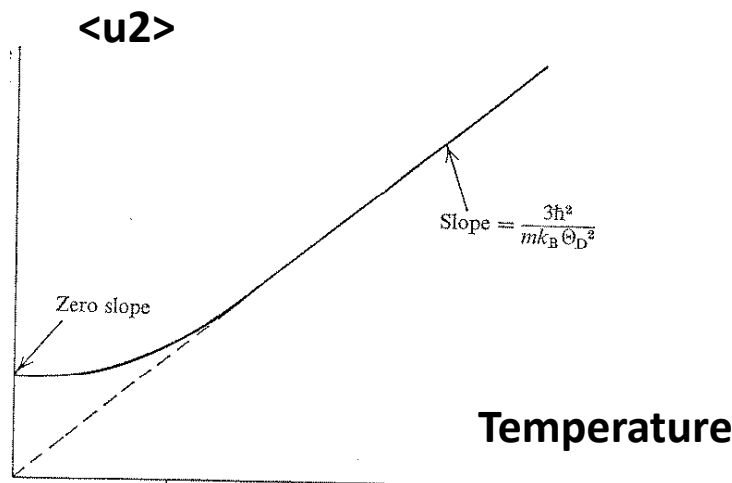
Atomic site symmetry may reduce the number of parameters, but often approximately 25 parameters per atom is needed in accurate studies. In least-squares refinement 10 reflections per parameter is advocated, i.e. 250 reflections per atom. Extensive data sets are necessary for charge density studies.

10,000 independent accurate reflections for 40 atom structure!

Solution : **Low-temperature and
short-wavelength synchrotron radiation**

$$T_{\text{harm,iso}} = \exp(-8\pi^2 \langle u_j^2 \rangle) (\sin\theta/\lambda)^2$$

The Debye approximation for atomic thermal motion as function of temperature gives a hint.
 $T \rightarrow 0$ K results in temperature factor $\rightarrow 1$.



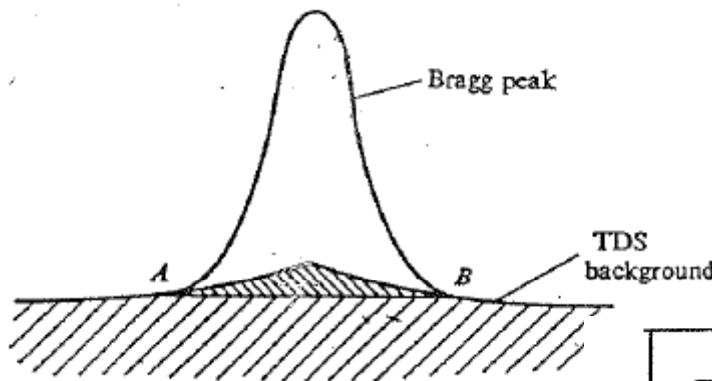
Approximate **intensity gain factors**
 by lowering temperature

	$\sin\theta/I$	$I(100 \text{ K})/I(290 \text{ K})$	$I(10 \text{ K})/I(100 \text{ K})$
1.0	100	5	
1.3	2 500	10	

Lowering temperature

- 1) gives more significant reflections and
- 2) increases accessible $\sin\theta/I$ range
- 3) makes anharmonic contributions insignificant,

Thermal Diffuse Scattering (TDS)

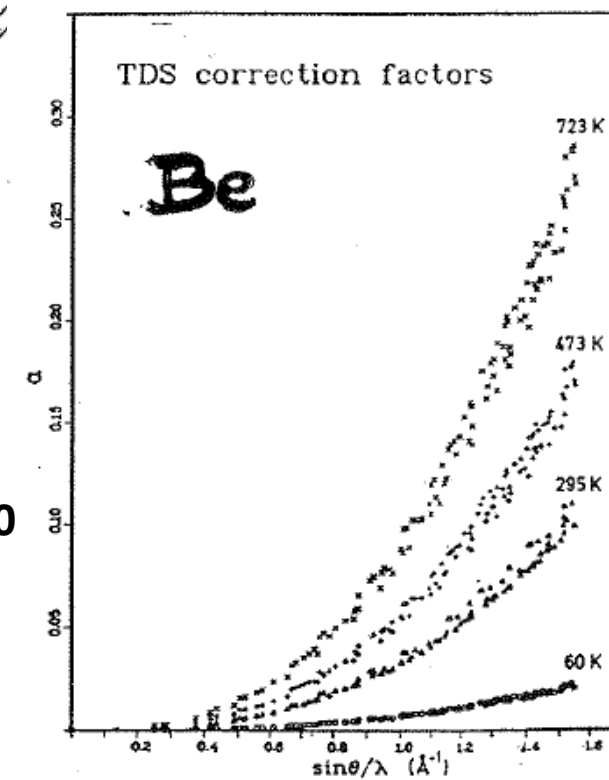


$$R(H)\text{meas}(T) = R(H)(T) (1+\alpha)$$

α is correction factor for first order TDS.

Can only be calculated
if elastic constants are known

TDS is at minimum at low temperatures →
better accuracy in measurements



Advantages of cryocrystallography

1) Reduced atomic thermal motion

- a) better resolution
- b) less TDS
- c) less anharmonicity

**more data
better data
simpler model**

2) Reduced radiation damage

The crystal lasts longer in the beam

The colder the better!

And then of course preferably use

SYNCHROTRON RADIATION

High brilliance, tunability and generally short wave lengths allows :

use of :

tiny crystals for less absorption and extinction generally, and

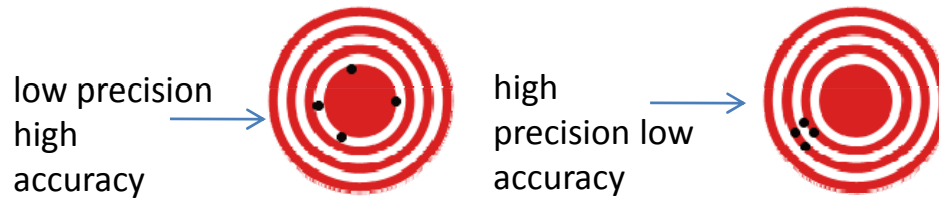
choice of :

short wavelength below absorption edges for heavy atoms

The ideal way to charge density data

The ideal experiment has the following ingredients

- ▶ Significant diffraction to high-angle ($(\sin(\theta)/\lambda)_{\max} > 1.0 \text{ \AA}^{-1}$)
- ▶ Spherical or face-indexed crystal
- ▶ Very low temperature (liquid He-flow or closed-cycle cryostat)
- ▶ High incoming intensity, eg. synchrotron X-ray source with high brilliance
- ▶ Neutron data for H-parameters (position and anisotropic adp)
- ▶ High accuracy as well as high precision (as in low R(int) from Sortav etc.)



How can we determine what we have?

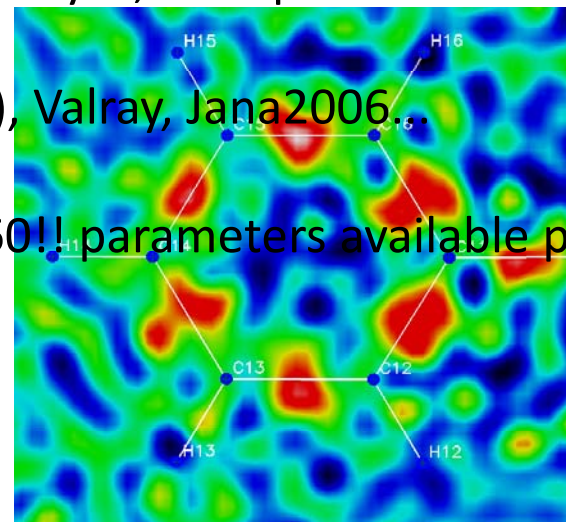
- ▶ Comparison with theoretical calculations
- ▶ Comparison of data from different sources and using different equipment, detectors...

Refinement approach

A general entry to charge density modeling

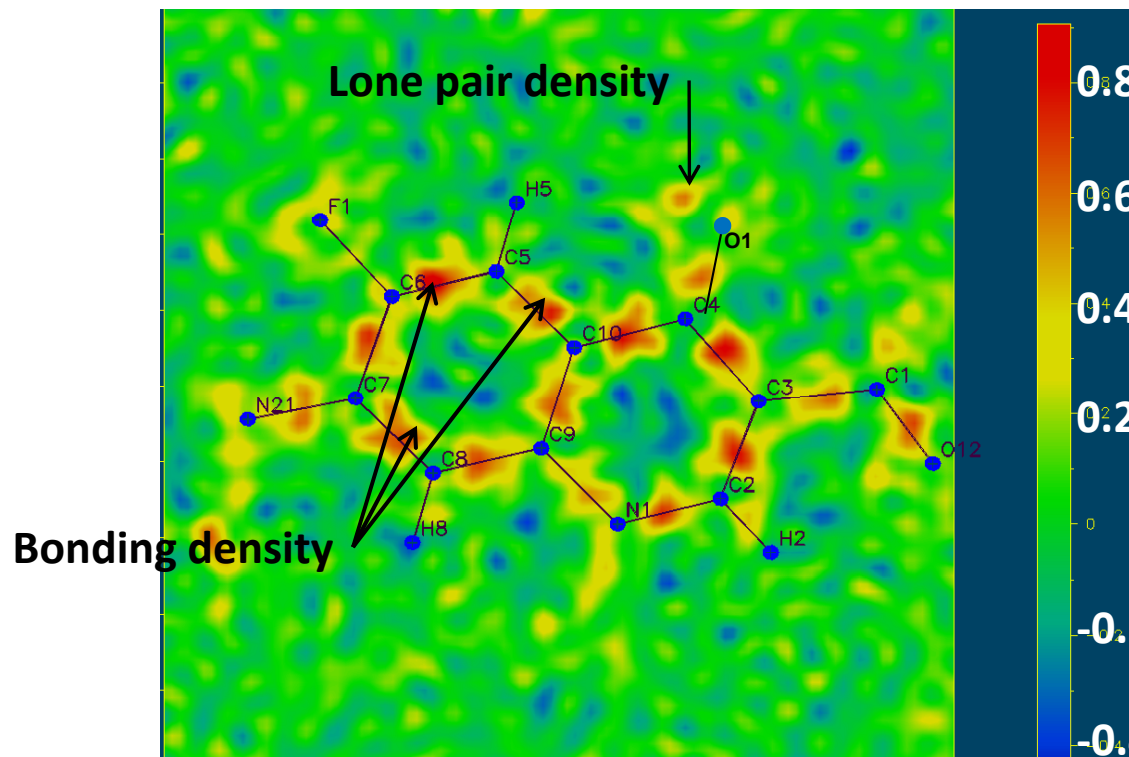
- ➡ As always, complete an IAM structure determination (SHELX or other)
- ➡ Study the Fourier difference maps from the above – do they show excess bonding density or other characteristic trends? If yes, the option is there.

- ➡ Specialised software is required: XD (WinXD), Valray, Jana2006...
- ➡ $3(xyz) + 6(U's) + 1(\kappa) + 25(\text{anharm}) + 25(P_{lm}'s) = 60!!$ parameters available per atom



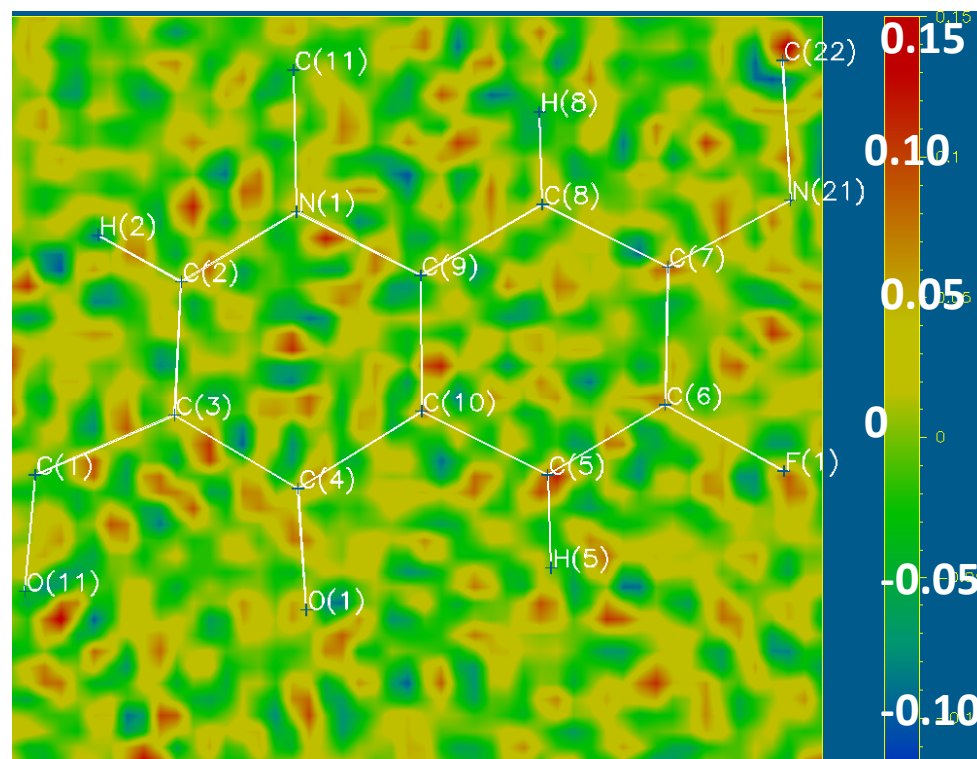
Any improvement of the fit?

IAM model: $\Delta F = (F(\text{obs}) - F(\text{calc}))$



Improvement

Multipole model: $\Delta F = (F(\text{obs}) - F(\text{calc}))$



Refinement details

A rough guide to charge density modeling

- ▶ Initiate with a refinement of the positional and thermal parameters using the high-angle data, typically maintaining a cut-off of at least 0.8 \AA^{-1} .

Refinement details

A rough guide to charge density modeling

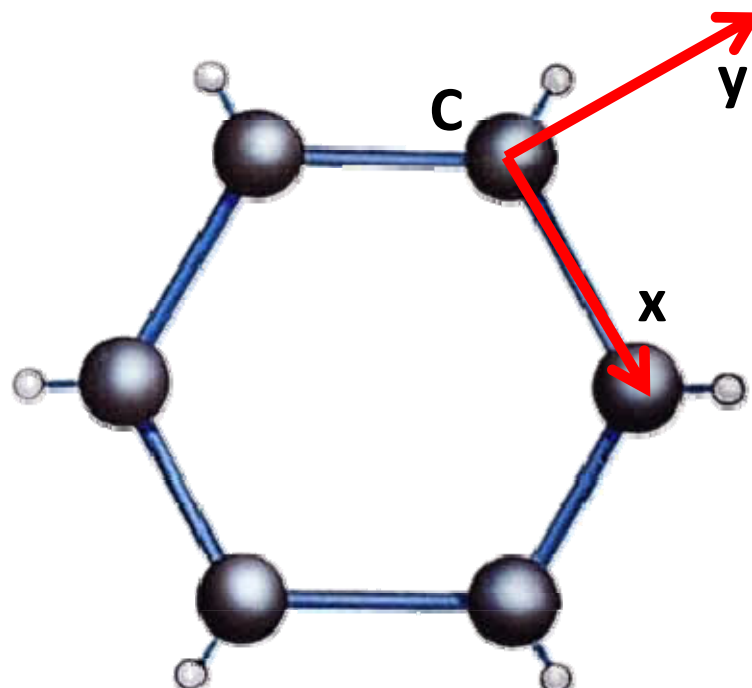
- ▶ Initiate with a refinement of the positional and thermal parameters using the high-angle data, typically maintaining a cut-off of at least 0.8 \AA^{-1} .
- ▶ Fix these parameters. Now start with a κ -refinement of κ and P_v .
- ▶ Make clever local coordinate systems & find any possible non-crystallographic symmetry elements to introduce constraints on the choice of refinable P_{lm} 's.

Local coordinate system

Choose for each atom
two neighbours to define
the LCS.

If, for instance, a mirror
plane is $\perp z$, then
selection rules apply:

1	any	all (l, m, \pm)
1	any	$(2l, m, \pm)$
2	$2\parallel z$	$(l, 2\mu, \pm)$
m	$m\perp z$	$(l, l-2\mu, \pm)$
$2/m$	$2\parallel z, m\perp z$	$(2l, 2\mu, \pm)$
222	$2\parallel z, 2\parallel y$	$(2l, 2\mu, +), (2l+1, 2\mu, -)$
mm2	$2\parallel z, m\perp y$	$(l, 2\mu, +)$
mmm	$m\perp z, m\perp y$	$(2l, 2\mu, +)$



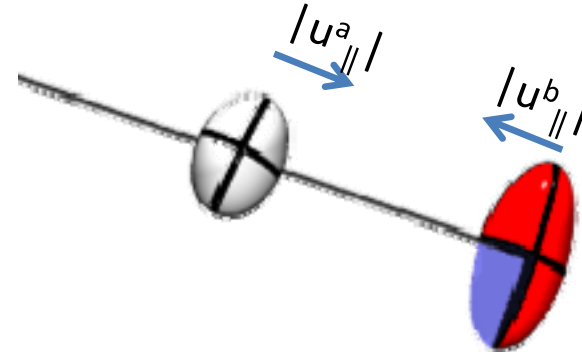
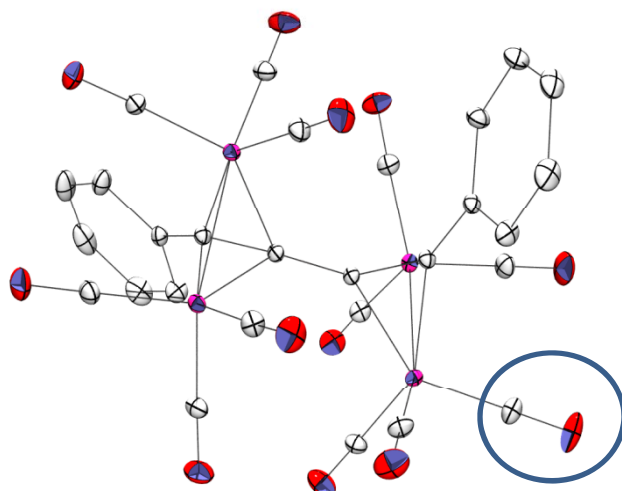
Refinement details

A rough guide to charge density modeling

- ▶ Initiate with a refinement of the positional and thermal parameters using the high-angle data, typically maintaining a cut-off of at least 0.8 \AA^{-1} .
- ▶ Fix these parameters. Now start with a κ -refinement of κ and P_v .
- ▶ Make clever local coordinate systems & find any possible non-crystallographic symmetry elements to introduce constraints on the choice of refinable P_{lm} 's.
- ▶ Introduce the multipoles in a sequence of refinement steps and examine the parameters for significance.
- ▶ Eventually include also κ' , although this may not converge or give large deviations from unity → KRMM

Validating the (final) model

► Hirshfeld rigid bond test

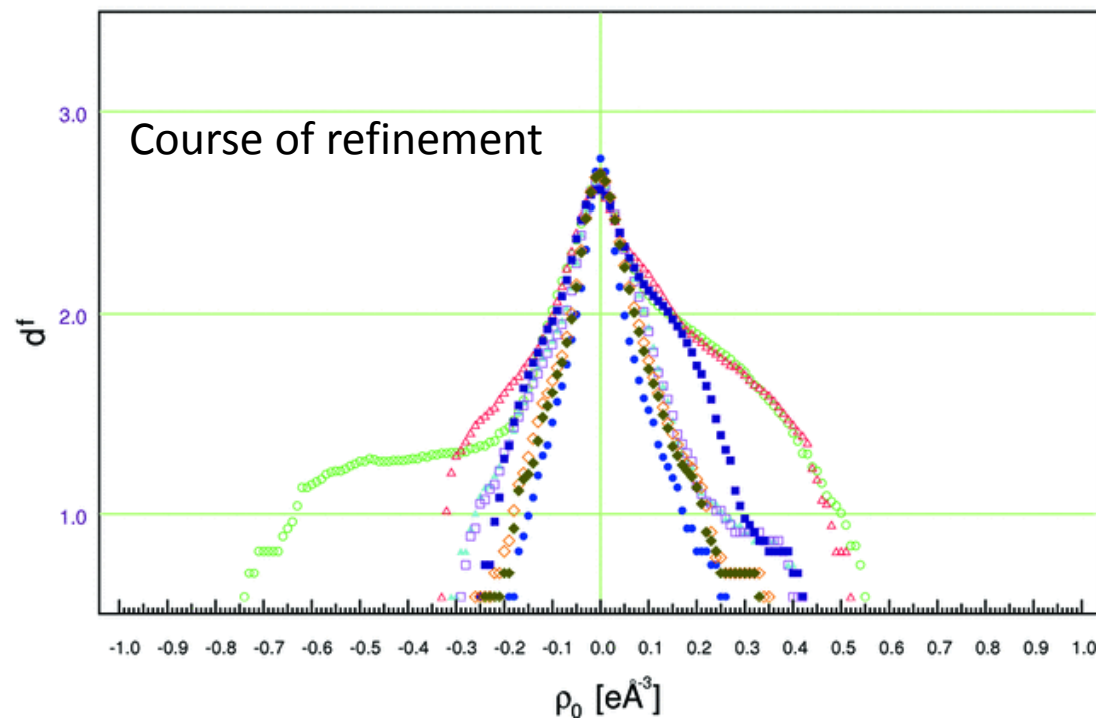


$$|u_a^{\parallel}| - |u_b^{\parallel}| \sim 0 (< 10^{-3} \text{ \AA}^2)$$

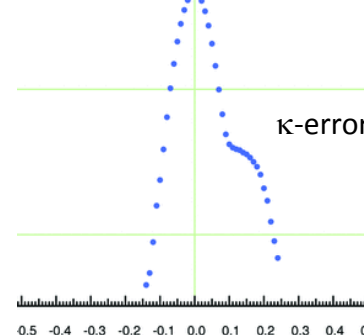
Hirshfeld, F. L. *Acta Crystallogr. Sect A*. **1976**, *32*, 239-244.

Validating the (final) model

► Analysis of the residual density in the unit cell – *program jnk2RDA*



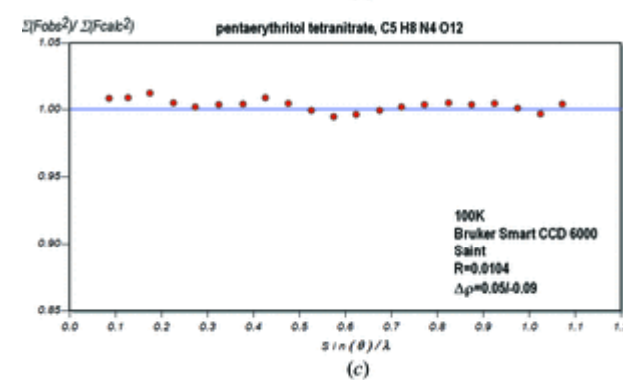
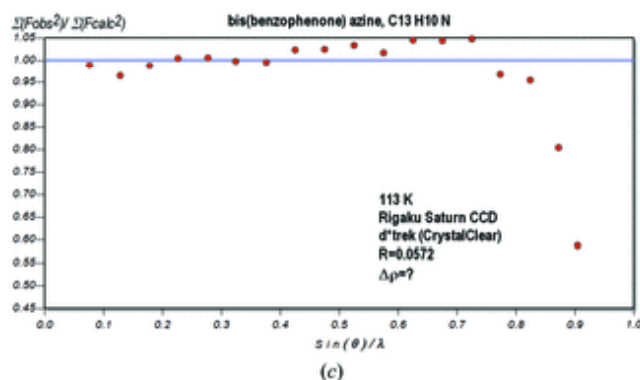
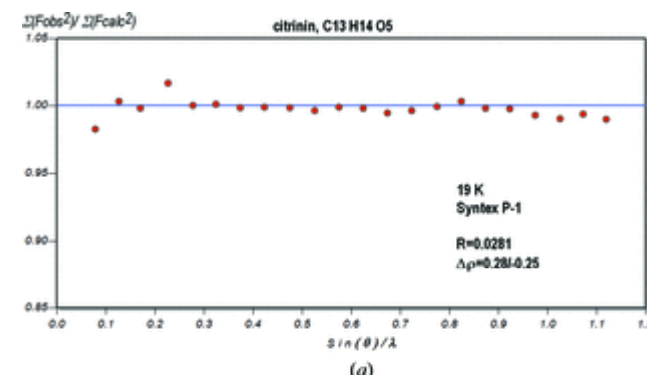
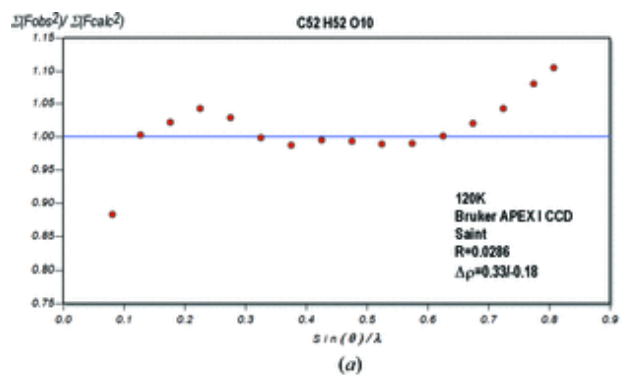
A number of systematic errors were introduced and their fingerprint in the fractal distribution plot was clarified.



Meindl, K.; Henn, J. *Acta Crystallogr. Sect A*. 2008, 64, 404-418.

Validating the (final) model

Shell like behaviour of $\sum F_{obs}^2 / \sum F_{calc}^2$

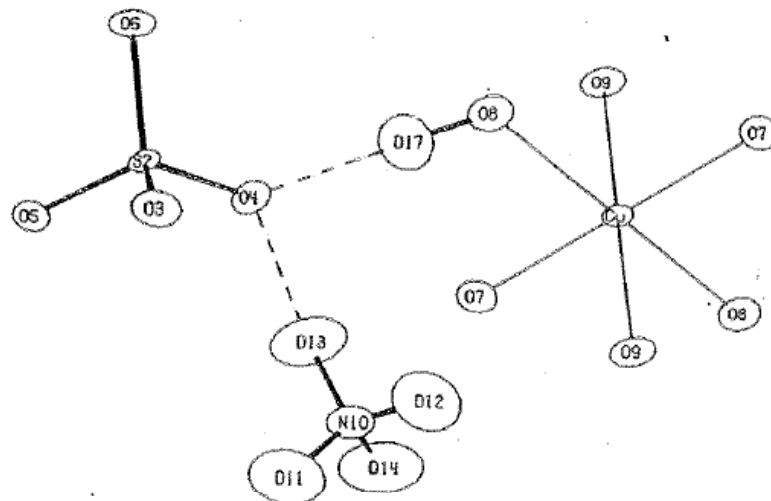


Zhurov, V. V.; Zhurova, E. A.; Pinkerton A. A. *J. Appl. Crystallogr.* 2008, 41, 340-349.

3d-electron population analysis

Copper Buttons' Salt

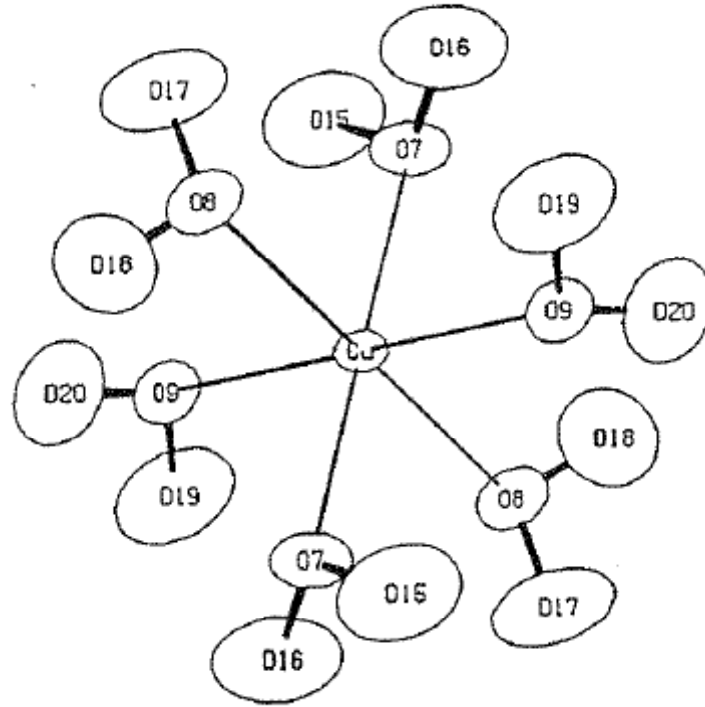
Copper Tuttons' Salt



Deuterated ammonium and sulphate groups are hydrogen bonded to Cu^{2+} ion, which is octahedrally hydrated by deuterated water molecules.

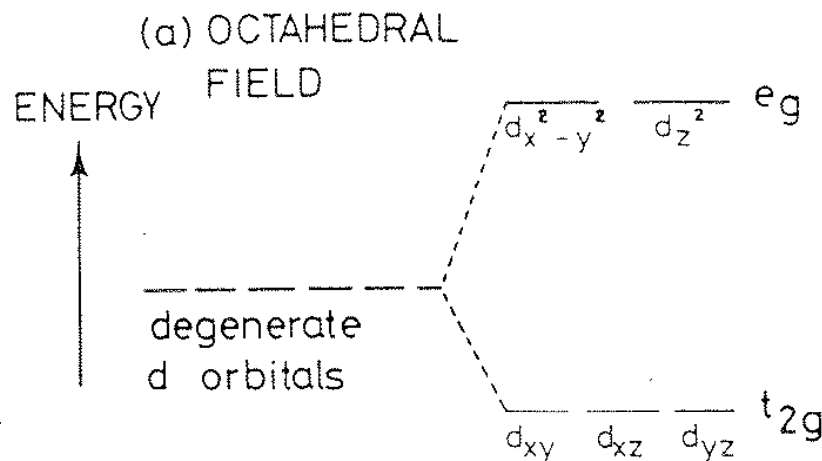
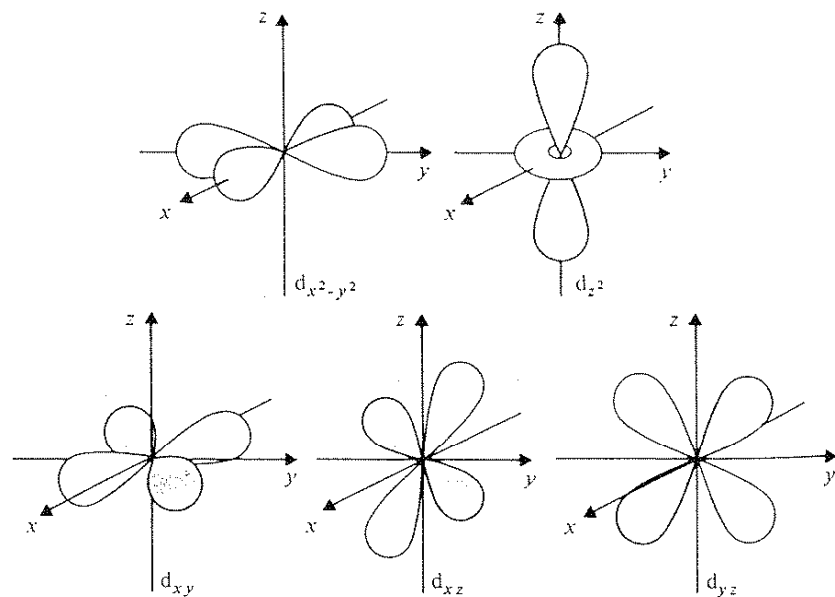
Geometry changes with temperature and pressure.

$\text{Cu}^{2+} (\text{D}_2\text{O})_6$ chromophore



$\text{Cu}^{2+} - (\text{D}_2\text{O})_6$ chromophore shows **Jahn-Teller distortion**.
Two Cu-O distances are significantly shorter than the third :

Cu-O7=2.081(6) Å, Cu-O8=2.242(7) Å, and Cu-O(9)=1.927(6) Å

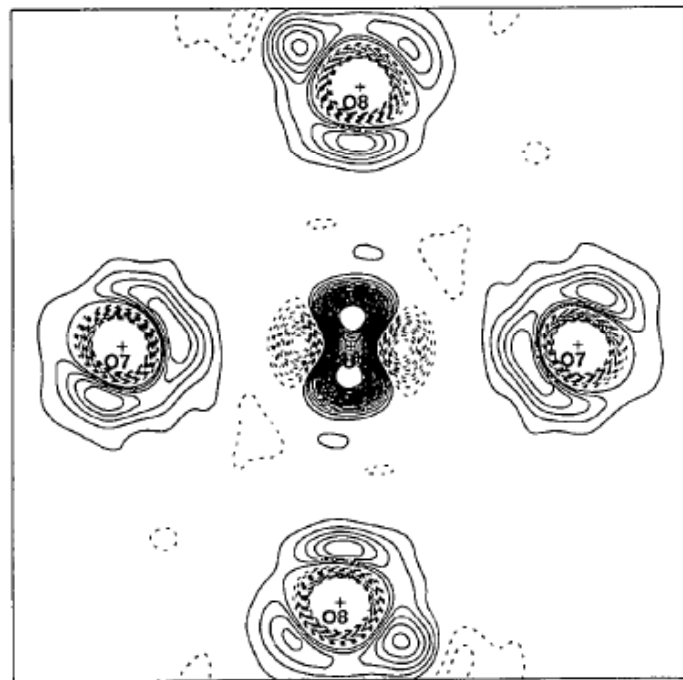


d-orbitals are energy split in an octahedral field

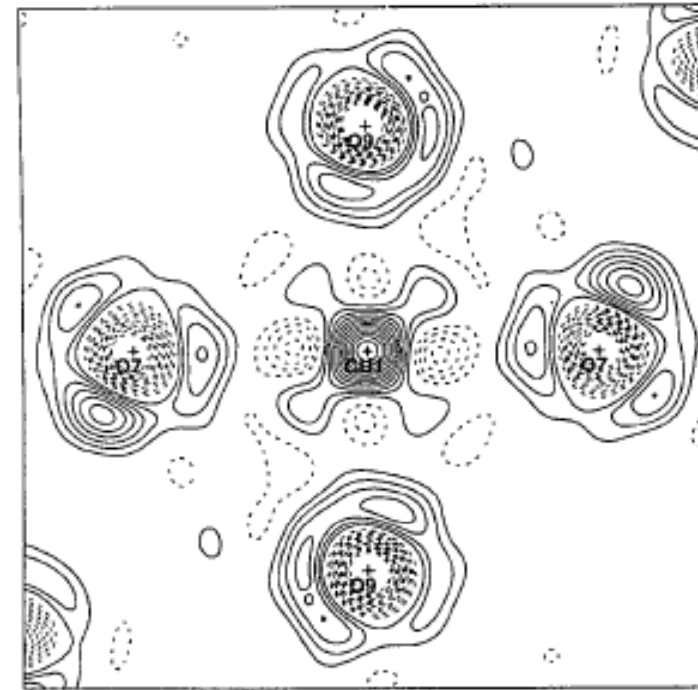
Cu^{2+} has 9 3d-electrons \rightarrow Expectation that $3d_{xy}$, $3d_{xz}$, $3d_{yz}$ and $3d_{z^2}$ orbitals are filled with electron pairs, while $3d_{x^2-y^2}$ is only partly populated

The long distance Cu-O8 must correspond to a fully occupied $3d_{z^2}$ pushing O8 away from Cu leaving $3d_{x^2-y^2}$ partly occupied .
This explains the shorter distances between Cu and O7 and O9.
The z direction is thus along Cu-O8, x and y directions along Cu-O7 and Cu-O9.

Model static deformation densities



z-axis vertical



x-y plane

Figgis, Iversen, Larsen and Reynolds, *Acta Cryst.* **1993**, *B49*, 794-806

3d-electron population analysis

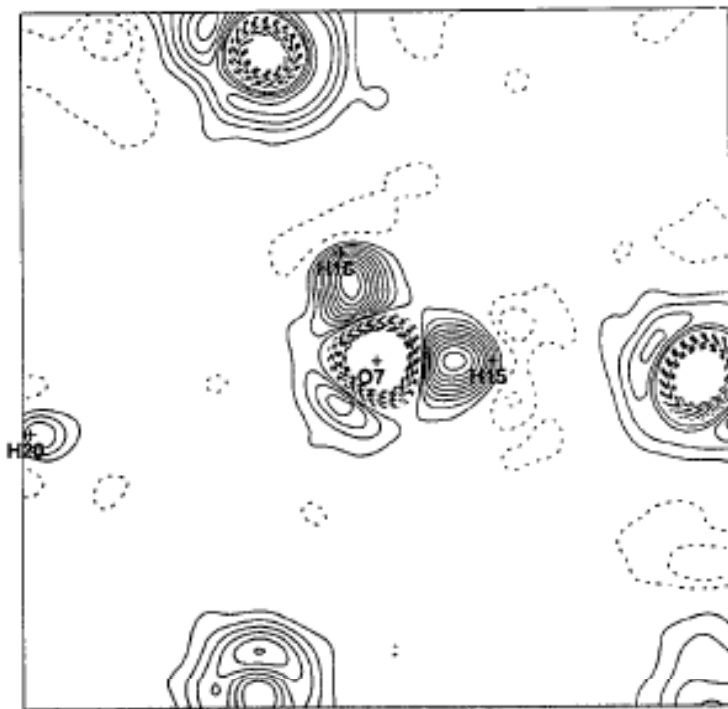
The static deformation maps of the deuterated Copper Tuttons' salt show:

- a) Water oxygen lone pairs directed towards Cu²⁺
- b) Flow of charge from SO₄²⁻ to Cu²⁺
- c) Deficiency of charge density in 3d_{x²-y²} orbital
- d) The z axis is directed from Cu²⁺ towards O8

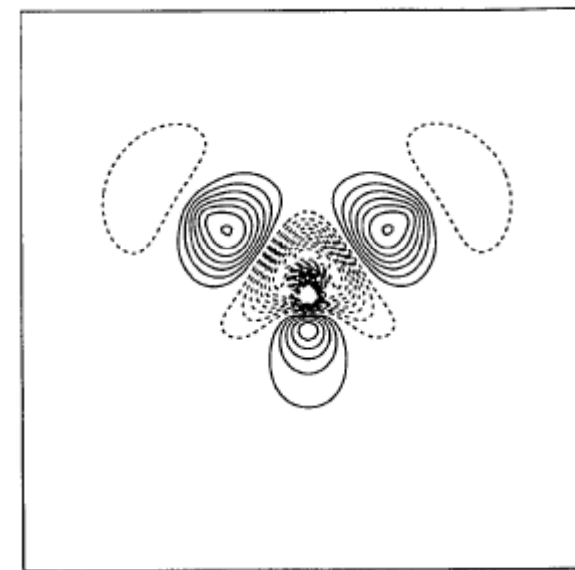
Valence function populations are in good accord with theoretical calculations
Chandler et al. *J. Chem. Soc. Faraday Trans.* **1992** 2, 88, 1961-1969.

	9 K	Theory
3d _{xy}	2.14(2)	1.95
3d _{xz}	2.02(2)	1.96
3d _{yz}	2.01(2)	1.96
3d _{x²-y²}	1.26(2)	1.23
3d _{z²}	2.07(2)	1.98
Total	9.50	9.08

Water molecules



Static deformation



Ab initio theoretical deformation

Almost quantitative comparison

Is it worth the effort? What else? Topological analysis!

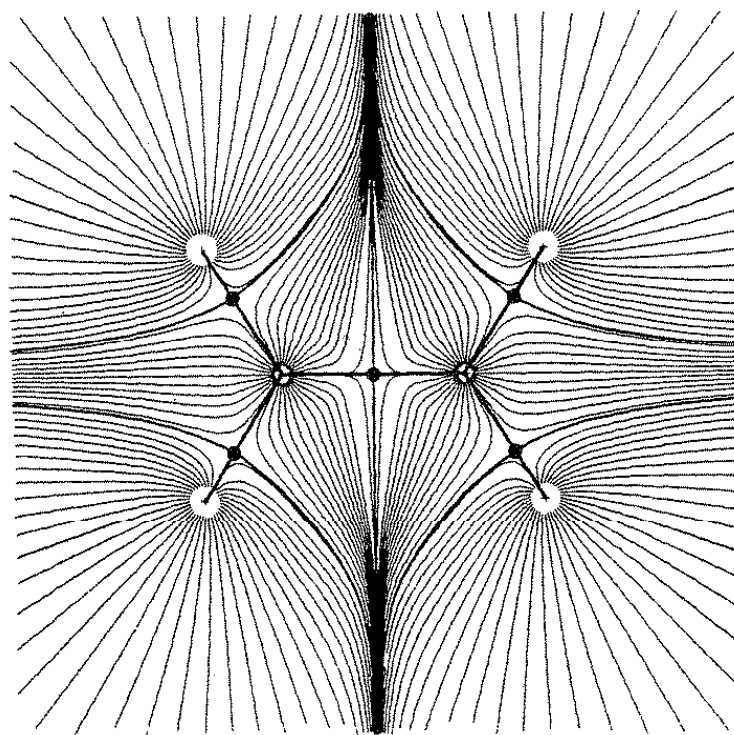
- When the experimental electron density is described analytically, its topology can be analysed in the same way as theoretically calculated densities are analysed using the Atoms in Molecules QTAIM (quantum theoretical atoms in molecules) theory by

Richard Bader

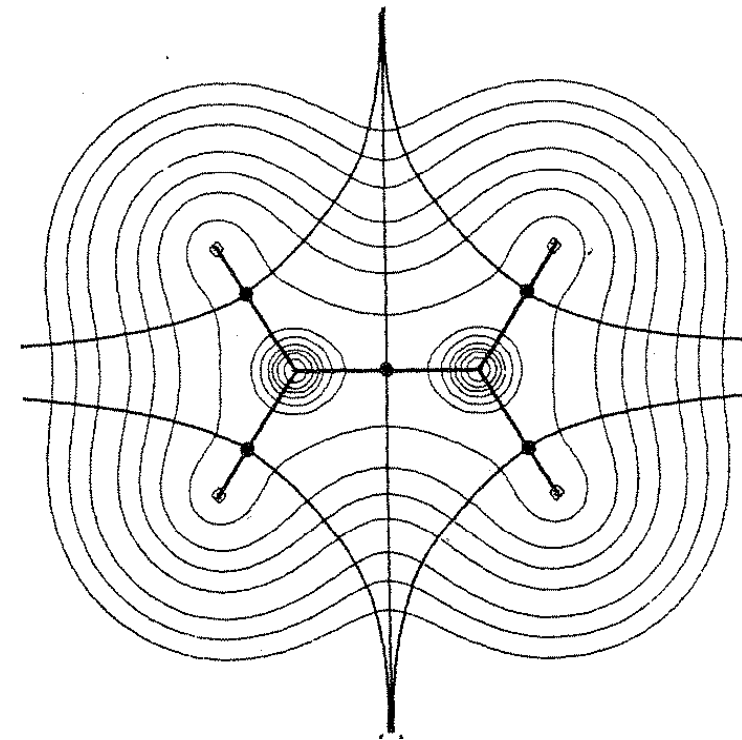
**THE INTERNATIONAL SERIES OF MONOGRAPHS ON CHEMISTRY:
ATOMS IN MOLECULES – A Quantum Theory
Clarendon Press Oxford – 1990**

Topological analysis opens possibilities for comparisons with a wide variety of experimental measurements

Topology of the C₂H₄, ethylene molecule



Gradient vector field $\nabla\rho(\mathbf{r})$
Attractor basins, critical points



Contour map of the charge density

Topological analysis of the electron density

- ✓ Zero-flux surface $\nabla\rho(\mathbf{r})\cdot\mathbf{n} = 0$ separates **atomic basins**, which each contains one and only one nucleus.
- ✓ **Critical points** where $\nabla\rho=0$.
- ✓ At the critical points, there are four possibilities for the algebraic sum of the eigenvalues , λ_i of $\nabla^2\rho$:
-3, -1, +1 or +3 corresponding to a **nucleus**, a **bond-**, a **ring-**, or a **cage-critical point**.
- ✓ Atomic properties can be calculated by integration over the atomic basin, for instance :

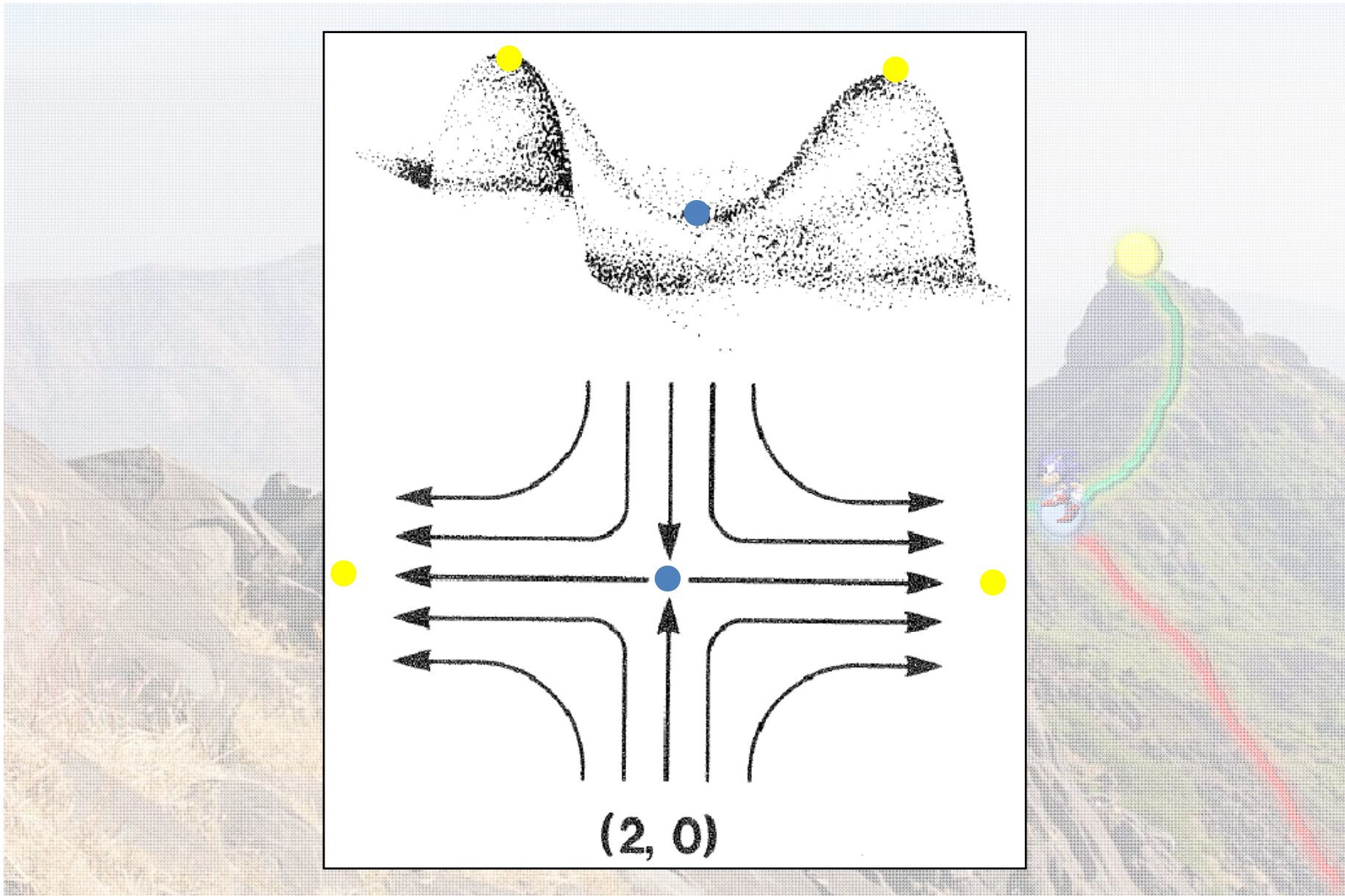
the atomic charge

and

the volume

$$q(\Omega) = N(\Omega) - Z = \int_{\Omega} \rho(r) d\tau$$

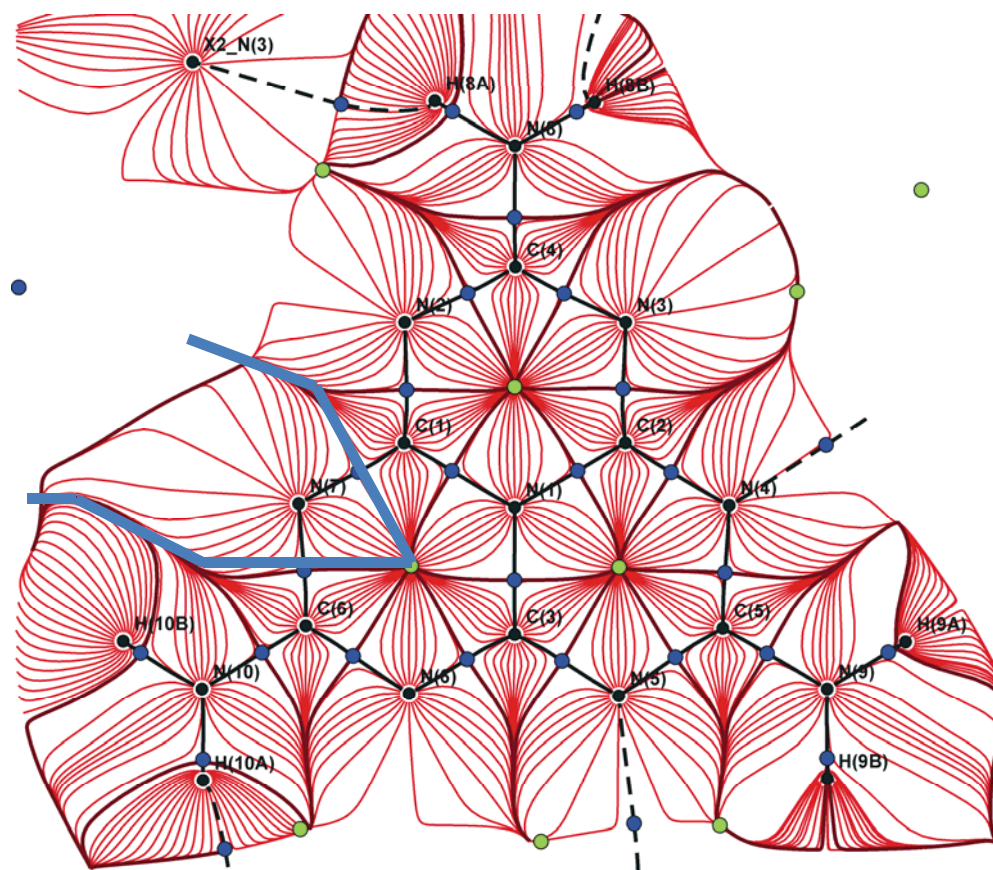
$$V(\Omega) = \int_{\Omega} d\tau$$



R. F. W. Bader; Atoms In Molecules, Clarendon Press, Oxford 1990

Atoms in Molecules partitioning

$C_6N_7(NH_2)_3$ – melem - in 2D



Physical and chemical characterizations

- Basic crystallographic analysis gives information on chemical composition, structural geometry and atomic thermal motion.
- Multipolar analysis can determine d-orbital populations for metal atoms.
- Topological QTAIM analysis furthermore allows calculation of
 1. Atomic volumes and charges
 2. Characterization of chemical interactions – chemical bonds
 3. Outer electronic moments: dipole moments, quadrupole moments etc
 4. Electric field gradients on the nuclear position – to be correlated with measured quadrupole splitting energy from Mossbauer spectroscopy
 5. Estimates of the crystal lattice energy

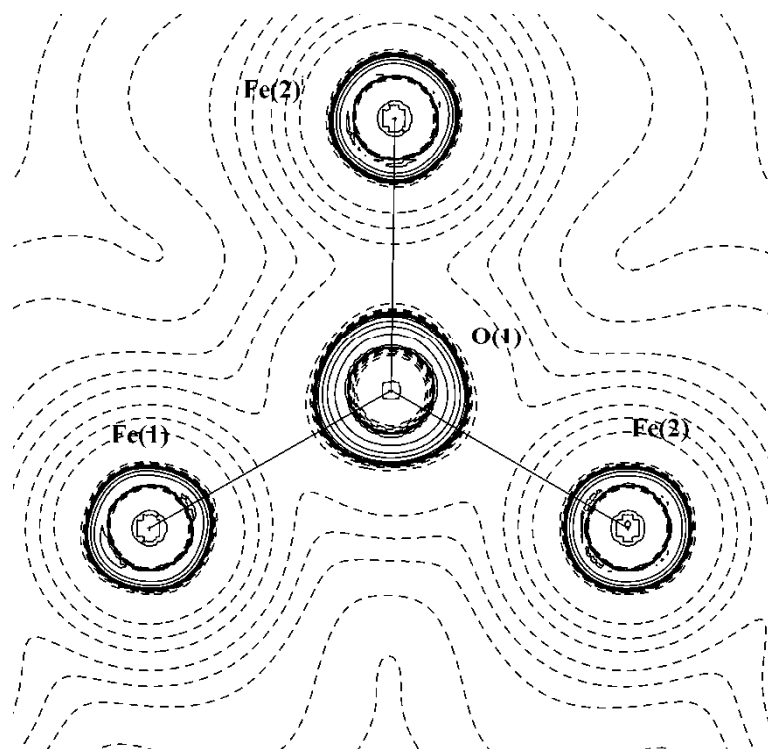
Characterization of chemical interactions

the negative Laplacian, $-\nabla^2\rho(r)$

Charge depletion

$$-\nabla^2\rho(r) < 0$$

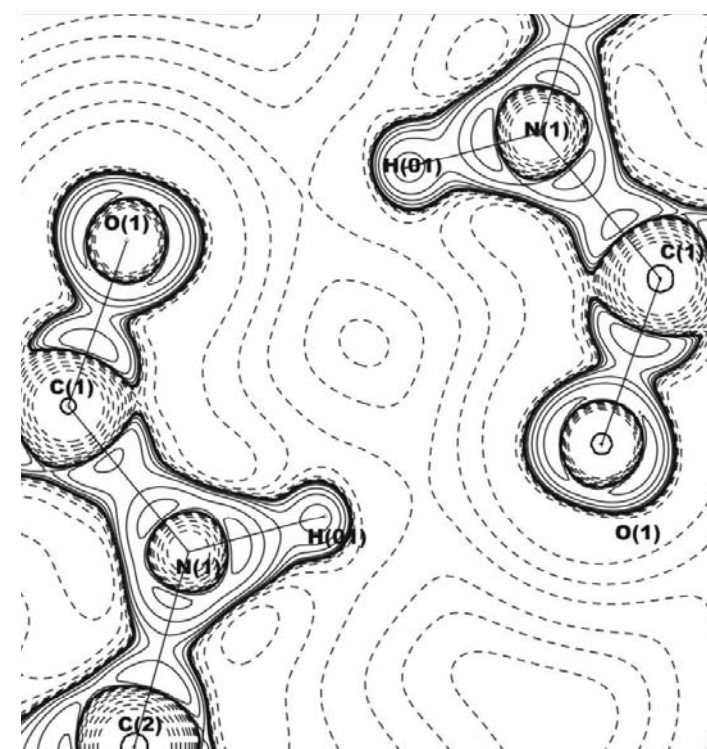
Ionic bonds



Charge accumulation

$$-\nabla^2\rho(r) > 0$$

Covalent bonds



Energy densities

- Energy densities can be estimated from the topological analysis using the expression by Abramov:

$$G(\mathbf{r}_{bcp}) = \frac{3}{10} (3\pi^2)^{2/3} \rho(\mathbf{r}_{bcp})^{5/3} + \frac{1}{6} \nabla^2 \rho(\mathbf{r}_{bcp})$$

- Based on results from neutron diffraction studies and the local virial theorem, Espinosa proposed a formula to derive the dissociation energy of a HB:

$$V(\mathbf{r}_{bcp}) = \frac{\hbar}{4m} \nabla^2 \rho(\mathbf{r}_{bcp}) - 2G(\mathbf{r}_{bcp})$$

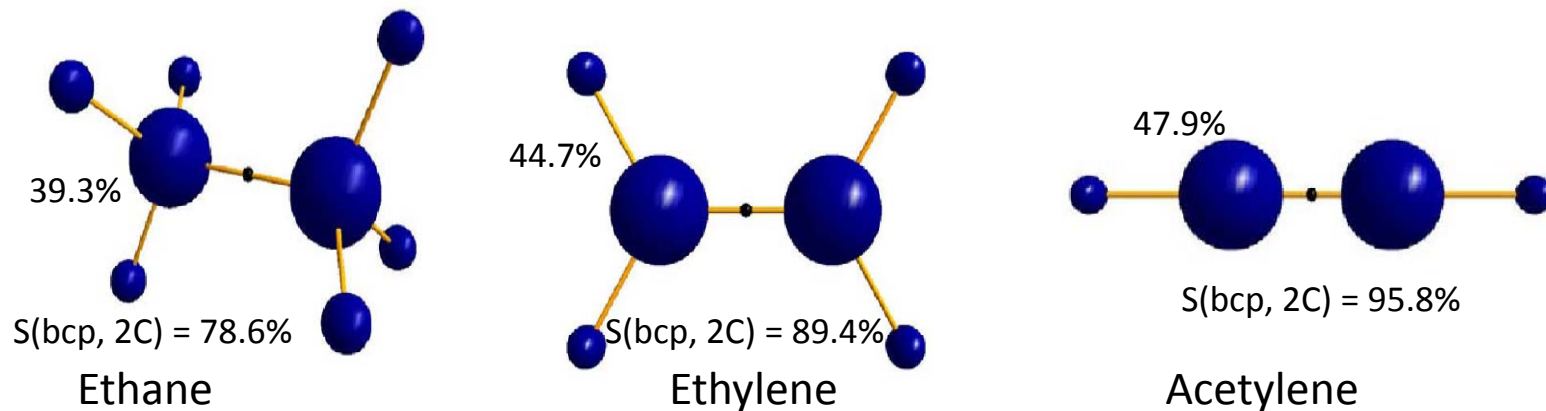
$$\mathbf{E}_{\text{HB}} = 0.5 * V(\mathbf{r}_{bcp})$$

Abramov, Yu. A. *Acta Cryst.* **1997**, A53, 264.
Espinosa, E. et al., *Chem. Phys. Lett.* **1998**, 285, 170.

Other descriptors

The source function, f. Inst. for characterization of hydrogen bonds

$$\begin{aligned}\rho(\mathbf{r}) &= \int_V -\frac{1}{4\pi|\mathbf{r} - \mathbf{r}'|} \nabla^2 \rho(\mathbf{r}') d\mathbf{r}' \\ &= \sum_{\Omega} \int_{\Omega} -\frac{1}{4\pi|\mathbf{r} - \mathbf{r}'|} \nabla^2 \rho(\mathbf{r}') d\mathbf{r}' \equiv \sum_{\Omega} S(\mathbf{r}, \Omega)\end{aligned}$$



Bader, R.F.W., Gatti, C. (1998), Chem. Phys. Lett. 287, 233-238.

C. Gatti in "The Quantum Theory of Atoms in Molecules: from Solid State to DNA and Drug Design", C. Matta and R. Boyd (Eds.), Wiley-VCH.

MORE EXAMPLES

first CoSb_3

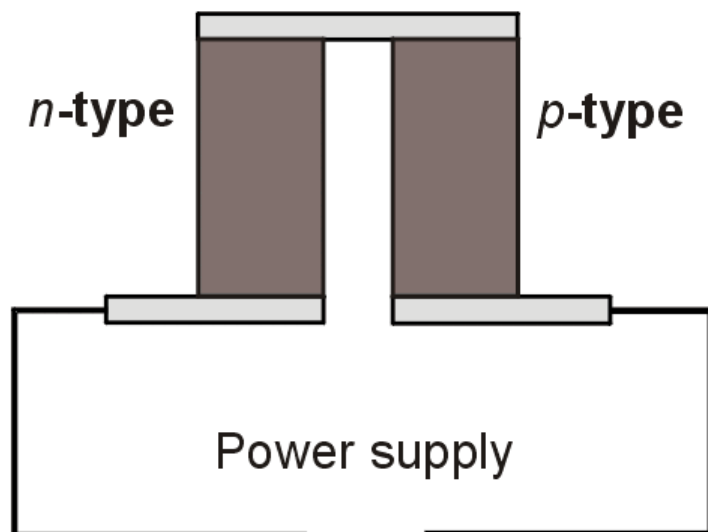
All made with XD – could be done with
other programs like JANA, Valray,
Molly etc.

THERMOELECTRIC MATERIALS

CoSb_3

Thermoelectrics

Active Cooling

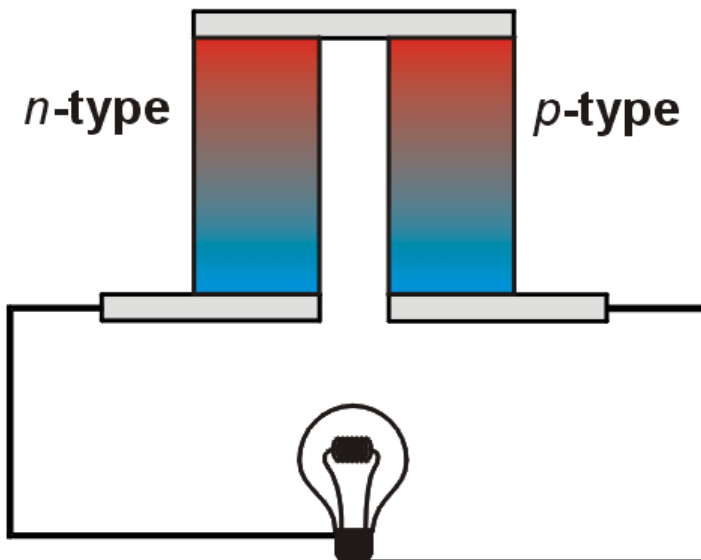


Peltier effect observed by
J. Peltier in 1834

Thermoelectrics

Thermoelectric Figure of Merit

Power Generation

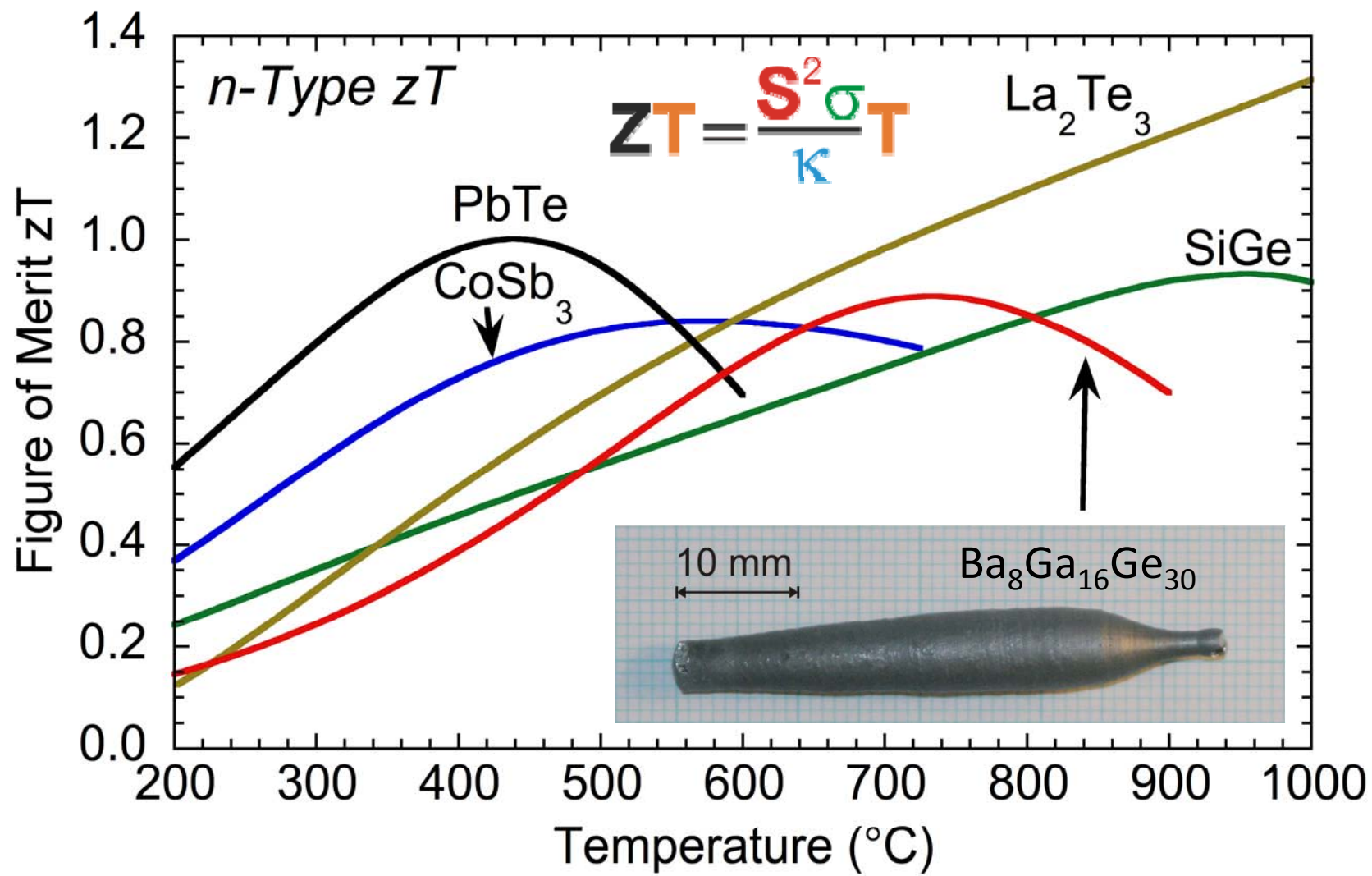


$$ZT = \frac{S^2 \sigma}{\kappa} T$$

Annotations for the Thermoelectric Figure of Merit equation:

- Seebeck coefficient (S) is indicated by a red arrow pointing to the first S in the numerator.
- Electrical conductivity (σ) is indicated by a green arrow pointing to the σ in the numerator.
- Thermal conductivity (κ) is indicated by a blue arrow pointing to the κ in the denominator.
- Temperature (T) is indicated by an orange arrow pointing to the T in the denominator.

In summary, we are looking for a;
Phonon Glass,
Electron Crystal



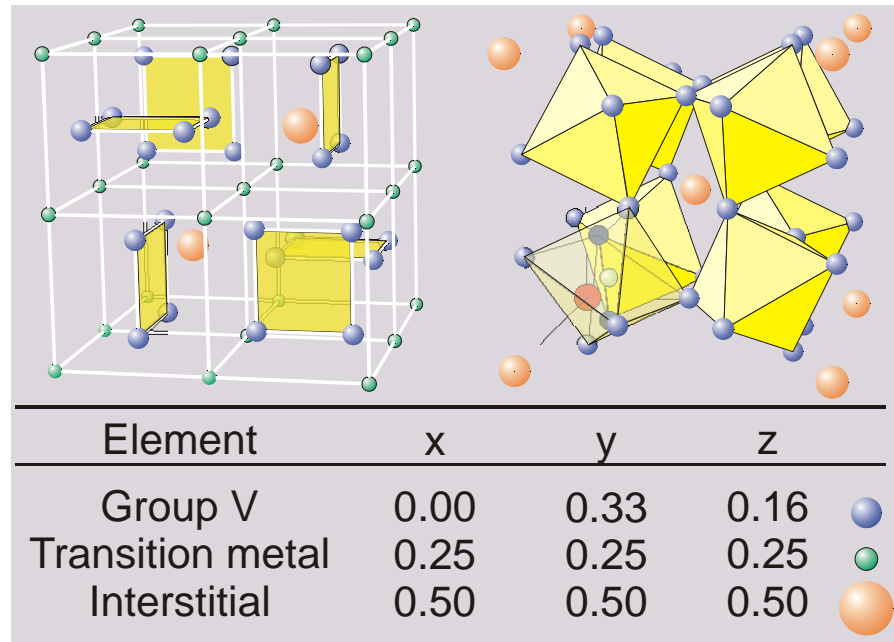
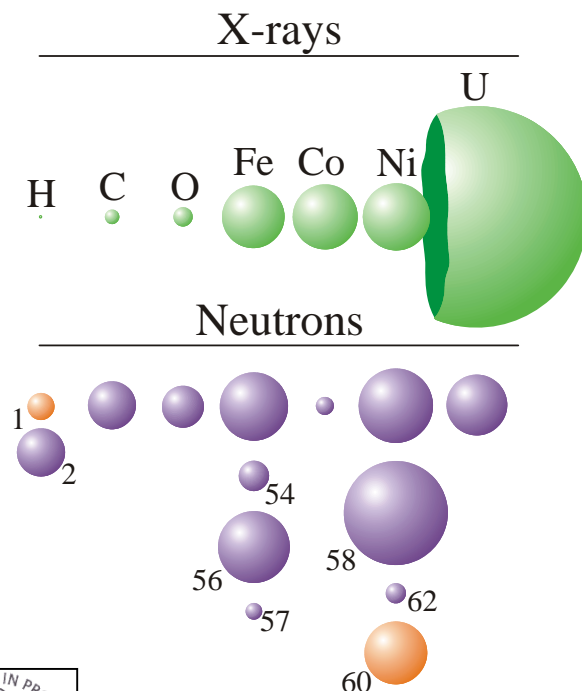
Doped CoSb₃

- Doping atoms – f. inst. La, Ba, Sn and Ni – improve the thermoelectric Figure of Merit primarily by decreasing the thermal conductivity.
- Theory: Bertini and Gatti *J.Chem. Phys.* (2004) **121**, 8983-8989
- Doping atoms can replace at atomic positions or go into interstitial position (0,0,0).
- Doping atoms can rattle in voids in the structure decreasing the lattice contribution to the thermal conductivity.
- Structural implications tested by neutron and X-ray synchrotron powder diffraction.

$\text{Co}_{(1-x)} \text{Ni}_x \text{Sb}_3$ Neutron diffraction

Neutron powder diffraction:
Investigate the Ni doping in the $\text{Co}_{(1-x)} \text{Ni}_x \text{Sb}_3$ system.

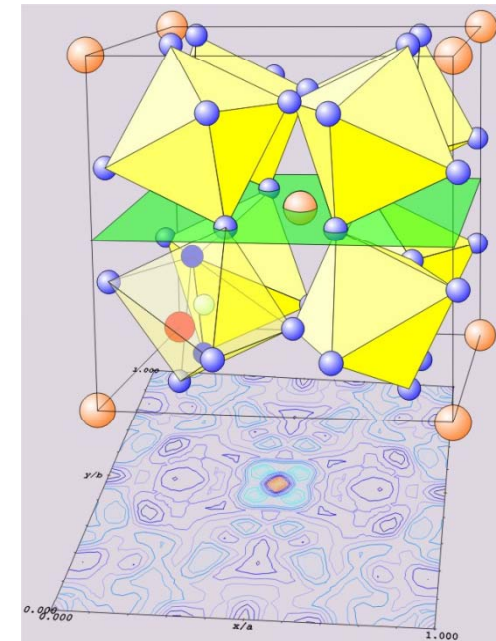
Ni and Co are almost indistinguishable by X-ray diffraction,
they differ a factor of ~ 16 in neutron diffraction.



$\text{Co}_{(1-x)} \text{Ni}_x \text{Sb}_3$ Neutron diffraction

Disagreement on stoichiometry between neutron powder diffraction and atomic absorption.

Interstitial sites 0.5 0.5 0.5 site appears to be occupied by Ni giving a formal stoichiometry of $\text{Ni}_{0.4}(\text{Co}_{7.8} \text{Ni}_{2.2})\text{Sb}_{30}$



The table shows the Ni content in %, and the mass density.

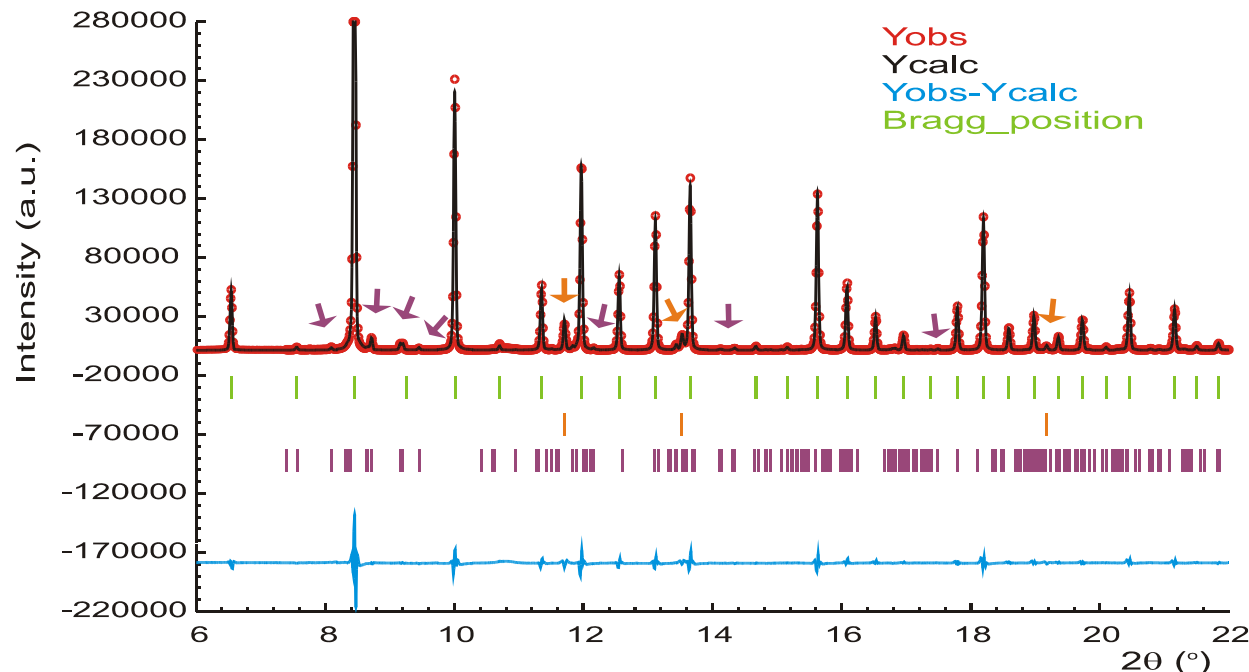
Sample	Framework	Framework + interstitial	Atomic absorption	Neutron density	Measured density
$\text{Co}_7 \text{Ni}_3 \text{Sb}_{30}$	0.22(1)	0.25(2)	0.30	7.643(5)	7.62(7)
$\text{Co}_8 \text{Ni}_2 \text{Sb}_{30}$	0.13(2)	0.15(3)	0.19	7.643(4)	7.9(1)
$\text{Co}_9 \text{Ni}_1 \text{Sb}_{30}$	0.04(2)	0.05(3)	0.08	7.633(3)	7.74(7)
$\text{Co}_{10} \text{Sb}_{30}$	0	0	0	7.646(4)	-

Additionally 1%-2% Ni can be added due to impurities



CoSb_3 Impurities

The high resolution and high intensity of the synchrotron radiation makes it possible to refine content of impurity.



Identified Phases:

CoSb_3 $a=9.02\text{\AA}$

fraction in weight % 96.4(3)

CoSb_2 $a=6.49\text{\AA}$ $b=6.37\text{\AA}$ $c=6.52\text{\AA}$ fraction in weight % 3.6(1)

CoN $a=3.57\text{\AA}$

fraction in weight % < 0.1



Conclusion – substituted Skutterudites

Neutron powder diffraction revealed:

- A deviation between intended Ni content and actual Ni content.
- Ni on the interstitial site.

Synchrotron powder diffraction:

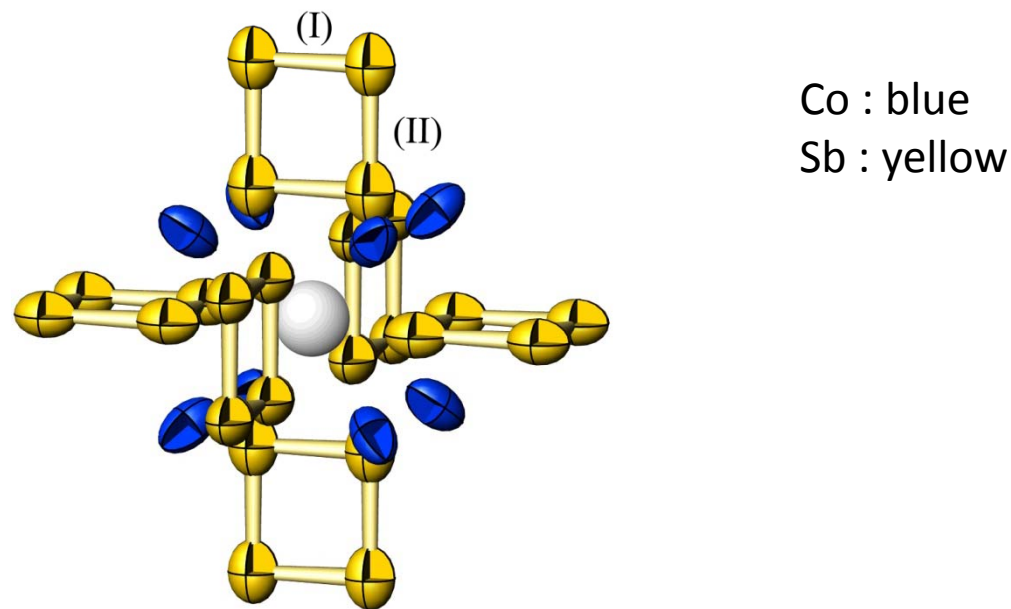
- Impurity phases could be quantified.

Follow-up work on pure CoSb₃:

- MEM density study from powder synchrotron X-ray data.
- Benchmark single crystal X-ray diffraction study including multipole modelling, and topological analysis.

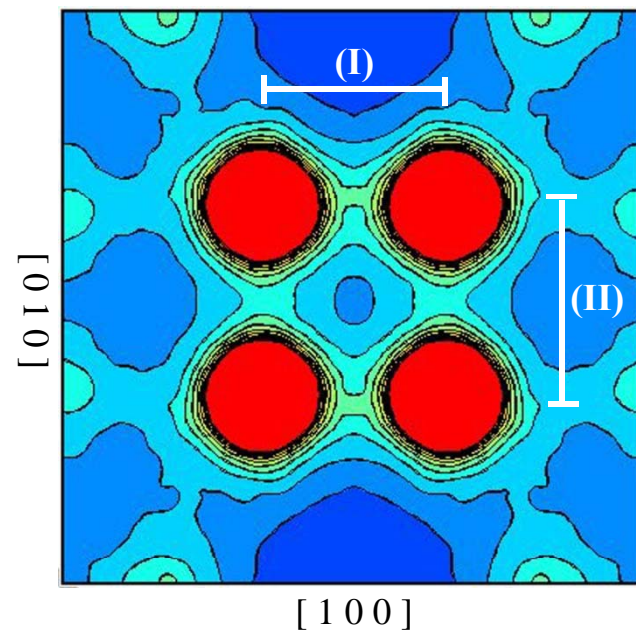


Spring-8 MEM results

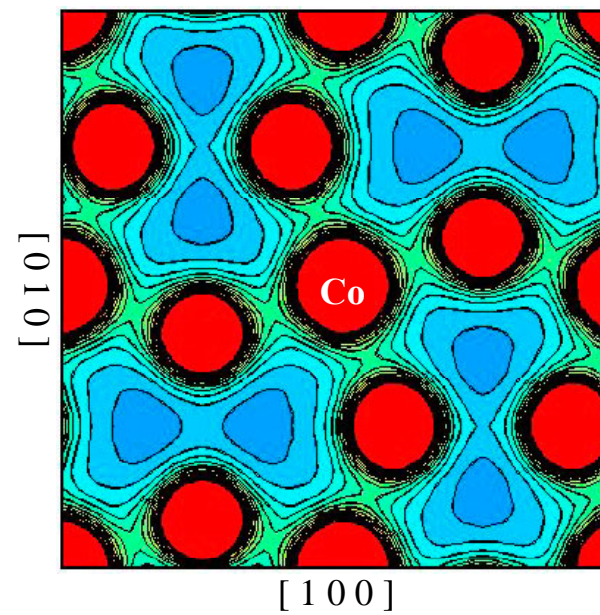


Ohno, Sasaki, Nishibori, Aoyagi, Sakata and Iversen,
Physical Review (2007) B76, 064119.

Spring-8 MEM densities



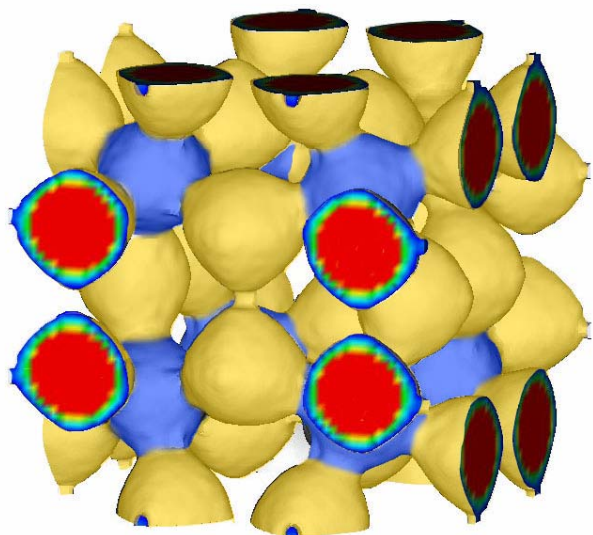
Sb-Sb (I) 2.86 \AA 0.50 e\AA^{-3}
Sb-Sb (II) 2.98 \AA 0.35 e\AA^{-3}



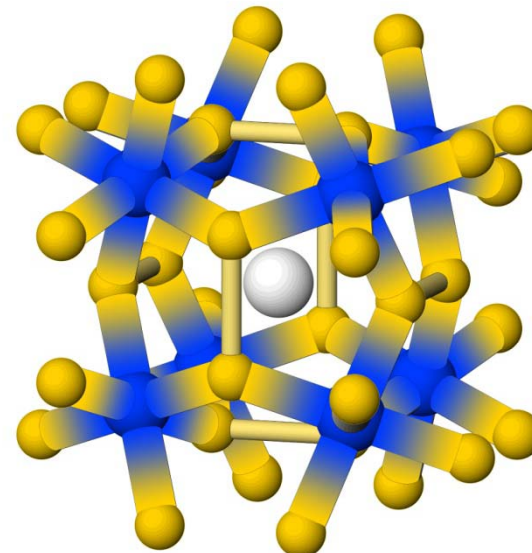
Co-Sb 2.53 \AA 0.52 e\AA^{-3}

CoSb_3 iso-surface plot and schematical model

Iso-surface at $0.40 \text{ e}\text{\AA}^{-3}$



$\text{Co}_8\text{Sb}_{12}$
Pentagonal Dodecahedron



Grey ball lies in centre of the void potentially occupied by rattling atoms

Pure CoSb₃ Skutterudite

Combined theoretical and experimental diffraction study.

CoSb₃, Mr=424.2,

cubic symmetry, space group *Im-3*

$a = 9.0165(1)$ Å at $T = 10$ K

Theory by Gatti et al., Milano

Single crystal X-ray diffraction study including multipole modelling, and topological analysis. Based on data collected at

Aarhus University (Larsen et al.),

University of Toledo (Pinkerton et al.) and at synchrotrons

APS (Yu-Sheng Chen) and

SPring-8 (Kunihisa Sugimoto)

Conventional X-ray diffractometers

HUBER, scintillation detector – Bruker APEX2 CCD
Radiation: Sealed tube AgKa - Rotating anode MoKa

Aarhus HUBER



Toledo APEX2



Advanced Photon Source Synchrotron

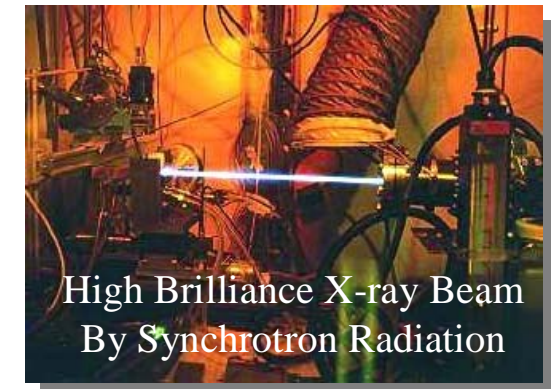
Argonne National Laboratory – Chem Mat Cars beamline

Radiation: $\lambda = 0.4201$ - Detector: Bruker AXS CCD



Super Photon ring 8GeV

SPring-8



High Brilliance X-ray Beam
By Synchrotron Radiation

Data comparisons

Data	T/ K	Xtal \emptyset μm	Cell a Å	$\sin\theta/\lambda$	λ	No meas	Unique	<N>	Extinc (1 3 0)	R _{int}
Huber	11	140	9.0082(7)	1.25	0.5608	33077	1071	30.9	50.5%	0.032
Toledo	20	-	9.0204(1)	1.32	0.7107	59113	1305	45.3	37.6%	0.034
APS (08)	16	15	9.0268(1)	1.19	0.4428	13553	2294	5.9		0.043
Spring-8	10	-	9.0206(3)	1.67	0.4117	56969	2559	22.3	1.5%	0.037
Spring-8 MEM	10	powder		1.8	0.4207	9256	1957	4.2	0	0.018

CoSb₃ – 49 model parameters

cubic symmetry, space group *Im-3 (# 204)*

Sb: 24g, *m-symmetry*

IAM : 0 y z, u₁₁ u₂₂ u₃₃ u₁₂; 15 anh.

CD : P_v P_{11±} P₂₀ P_{22±} P_{31±} P_{33±} P₄₀ P_{42±} P_{44±} κ' κ''

Co: 8c, -3 symmetry, x = y = z = 0.25;

$$u_{11} = u_{22} = u_{33}; \quad u_{12} = u_{23} = u_{13}$$

IAM : u₁₁ u₁₂

CD : P_v P₂₀ P₄₀ P_{43±} κ' κ''

Besides scale factor and extinction parameter

In total: 38 (Sb) + 9 (Co) + 2 = 49 parameters.

Parameter comparisons

	Aarhus	Toledo	APS (08)	Spring-8 (09)	Spring-8 (MEM)
Coordinates					
x, y, z(Co)	$\frac{1}{4}, \frac{1}{4}, \frac{1}{4}$				
X(Sb)	0	0	0	0	0
Y(Sb)	0.33542(2)	0.33544(2)	0.335222(4)	0.335225(5)	0.33510(1)
Z(Sb)	0.15780(2)	0.15778(2)	0.157864(4)	0.157858(5)	0.15805(1)
Thermal parameters					
U11(Co)	0.00218(9)	0.00229(9)	0.00235(2)	0.00228(1)	0.00289(3)
U12(Co)			0.00005(2)	0.00005(1)	0.00097(3)
U11(Sb)	0.00181(6)	0.00192(7)	0.00200(1)	0.00200(1)	0.00205(1)
U22(Sb)	0.00233(6)	0.00249(7)	0.00240(1)	0.00246(1)	0.00393(2)
U33(Sb)	0.00202(6)	0.00216(6)	0.00217(1)	0.00220(1)	0.00246(2)
U23(Sb)			0.00009(1)	0.00011(1)	0.00000(1)

Topological analysis of the multipole models

	Spring-8			theory	
	dist Å	ρ	$\nabla^2\rho$ $e\text{\AA}^{-3}$	ρ	$\nabla^2\rho$ $e\text{\AA}^{-3}$
Co-Sb	2.53	0.41	1.82	0.39	1.28
Sb-Sb (I)	2.86	0.33	0.56	0.50	-1.61
Sb-Sb (II)	2.97	0.33	0.51	0.47	- 0.86

Density profiles for Sb-Sb(long) interaction

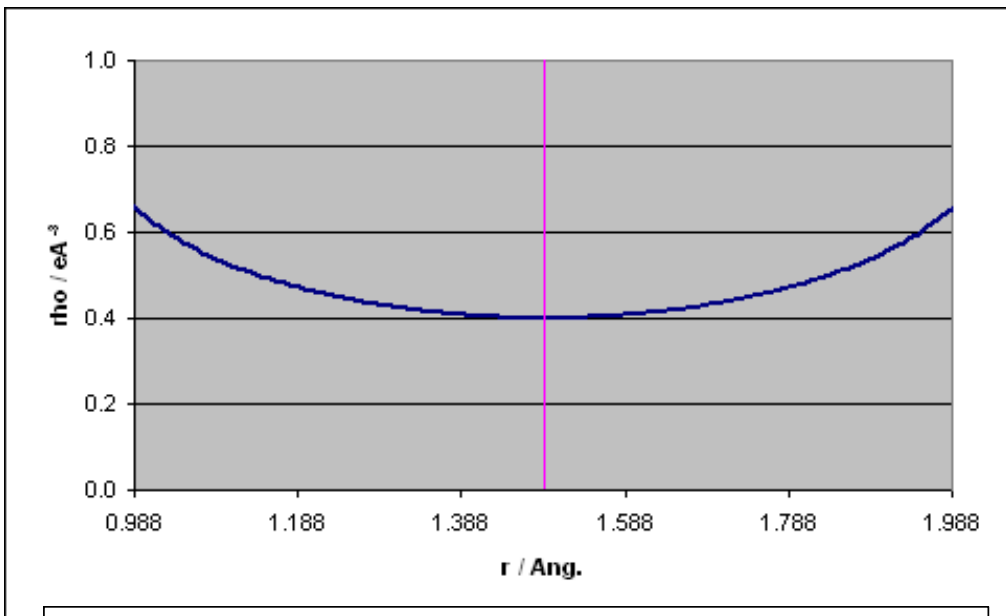


Figure 2a. ρ profile of Sb-Sb (long) interaction.

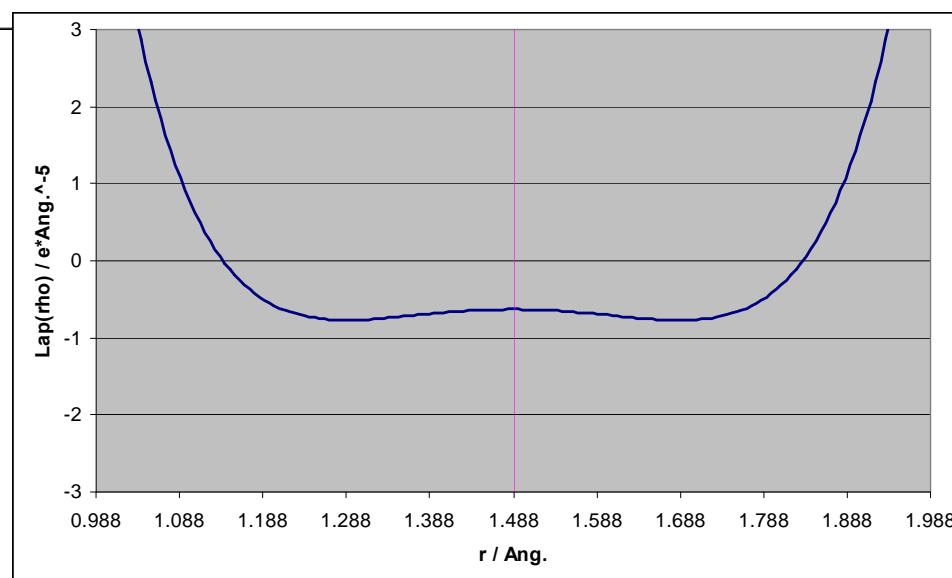
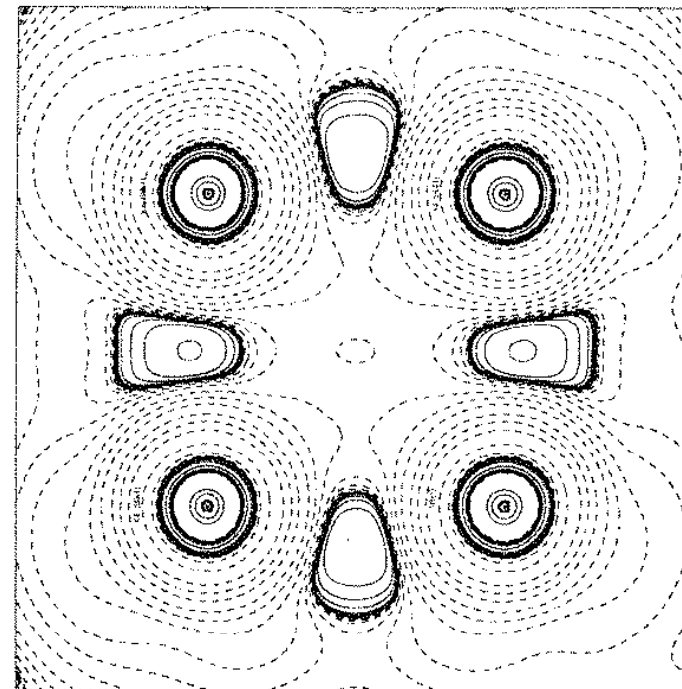
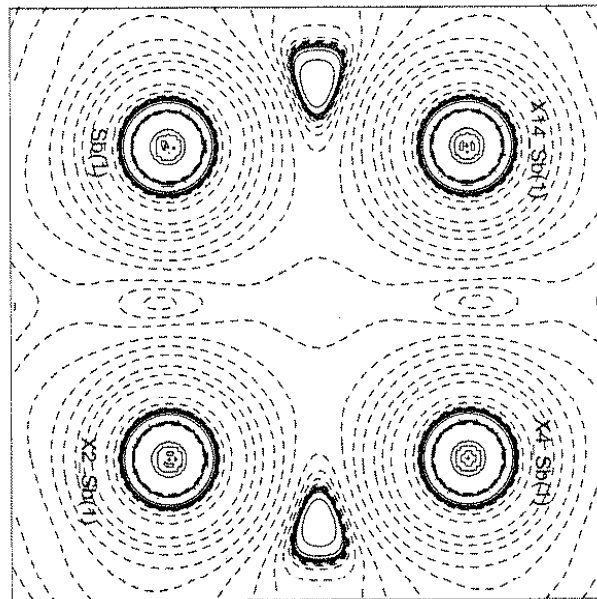


Figure 2b. $\nabla^2\rho$ profile of Sb-Sb (long) interaction.

Maps of the negative Laplacian in the Sb_4 plane

Theory (Gatti,Milano)

Spring-8 (2009)



State of affairs

Single crystal results from **Aarhus**, **Toledo**, **APS** and **Spring-8** – positional and thermal parameters agree perfectly, density parameters almost.

Most thermal parameters of Spring-8 powder MEM study deviate very significantly from single crystal results.

Electron Diffraction measurements of low-order structure factors would be desirable.

Comparison of topological measures for experiment and theory indicate **B3LYP/3-21G** as best theoretical model.

Calculating Bader atomic charges, energies and topological classification of bonds, etc. is next.

Benchmark CoSb_3 study.

Some Conclusions

Conventional data: Compare well – although rotating anode gives relatively more significant weak intensities.

Synchrotron data. VASTLY increased number of unique reflections . Strongly decreased extinction.

Spring-8 powder diffraction (BL02B2 beamline). MEM; very good qualitative electron density description, but

Spring-8 single crystal study (BL02B1 beamline). Most extensive and superior for multipolar and topological analysis.

Conclusions

- The experimental charge density method can give otherwise unattainable information on a wide variety of chemically interesting compounds
- Synchrotron data can be imperative
- A whole new array of properties are available through the use of QTAIM
- Very low temperature is strongly recommended
- Charge density modeling is “just” advanced structure refinement – but it requires extreme care in data acquisition and data analysis

Acknowledgements

Aarhus Charge Density People:

Bo Brummerstedt Iversen
Jacob Overgaard

Henrik F. Clausen
Mads R. V. Jørgensen
Rasmus D. Poulsen
Mette S. Schmøkel